Electronic Research Archive

ERA, 31(9): 5362–5395.
DOI: 10.3934/era.2023272
Received: 09 June 2023
Revised: 23 July 2023
Accepted: 24 July 2023
Published: 31 July 2023

http://www.aimspress.com/journal/ERA

Research article

A comparative analysis of the robustness of multimodal comprehensive transportation network considering mode transfer: A case study

Yongtao Zheng[1,2,3], Jialiang Xiao[1,2,3], Xuedong Hua[1,2,3], Wei Wang[1,2,3,*] and Han Chen[4]

[1] Jiangsu Key Laboratory of Urban ITS, Southeast University, Nanjing 211189, China
[2] Jiangsu Province Collaborative Innovation Center of Modern Urban Traffic Technologies, China
[3] School of Transportation, Southeast University, Nanjing 211189, China
[4] College of Art & Design, Nanjing Forestry University, Nanjing 210037, China

* **Correspondence:** Email: wangwei_transtar@163.com; Tel: +8617327750529.

Abstract: China has built a nationwide transportation network, but there needs to be a smooth connection and transfer between different modes. Five networks are constructed to explore the characteristics of a multimodal comprehensive transportation network (CNet) in Jiangsu Province based on the optimized modeling method and multisource data. Statistical and robustness characteristics are analyzed for CNet and other single-mode networks including the highway, railway, navigation channel and airway networks (HNet, RNet, NNet and ANet, respectively). The research results show following: (i) In Jiangsu, CNet, HNet, RNet and NNet are not scale-free networks and do not have small-world properties. However, ANet is the opposite. (ii) The five networks in Jiangsu are robust to the random attack and their robustness changes during the attack. However, their robustness is different under different calculated attacks. For all attack strategies, CNet is the most robust. (iii) In Jiangsu, the three optimized methods enhance the robustness significantly. The network failure is delayed by 12.34, 2.79 and 2.44%, respectively. The average connectivity degree is improved by 265.69, 52.95 and 32.54%, respectively. The more hubs there are with powerful transfer capacity, the stronger the network robustness. The results reveal the key points of the construction of a multimodal comprehensive transportation system and can guide the design and optimization of it.

Keywords: comprehensive transportation system; network construction; mode transfer; robustness analysis; comparative analysis

1. Introduction

The multimodal comprehensive transportation network (CNet) is important to the social economy. The transit hub is a key part of CNet for its function of connecting different transportation modes. Although a nationwide transportation infrastructure network has been built, China still lags in the United Nations' logistics index [1]. One important reason is that the transfer capacity of transit hubs is insufficient.

Robustness is an important property of the system to resist interference. To maintain operation, CNet needs to be robust. Because of its importance, the transit hub is more easily damaged and the negative influence is more serious. Therefore, two questions need to be considered during the stages of planning, construction and management if a robust CNet is needed. One is how to evaluate the robustness of CNet accurately considering the transfer function of the hub. Another is how to enhance the robustness of CNet based on the optimized hub.

Whether evaluating or enhancing, the research needs to focus on reality. Only in this way can conclusions and suggestions of important practical significance be drawn. First, the network model should accurately reflect reality. Otherwise, the evaluation results of robustness may be biased. Second, the basic statistical characteristics of networks should be researched, such as scale-free and small-world properties. It is beneficial to understand the state of the network. Third, it is necessary to perform a comparative analysis of how the optimized hub affects robustness. It is helpful for engineers to make the improved scheme.

Based on these objects, Jiangsu Province is selected as the case study. It is one of China's most economically powerful provinces. It also has a complete and powerful network system of multimodal comprehensive transportation. However, the issue of insufficient transfer capacity persists. Therefore, the CNet in Jiangsu can reflect its characteristics when used throughout China.

Generally, this paper has four contributions. First, the differences in statistical characteristics among CNet and single-mode networks are analyzed. We point out the features and explain the reasons for the degree distribution, scale-free and small-world and spatial scale when the CNet considers mode transfer. Second, the robustness of CNet and single-mode networks is compared. We use some indicators to show the structure failure process under four attack modes and compare the differences between CNet and other networks. Third, the robustness of four kinds of CNets is comparatively analyzed. We note how much the robustness of the CNet can be improved, which is modeled by the method proposed in this paper. We also show the improvement tendency caused by the number of optimized transit hubs. It also demonstrates the validity of our modeling method. Fourth, some suggestions from the planning, construction and management points of view are proposed. The suggestions are about the number of hubs and the design of transfer channels. We propose notification when evaluating the robustness of a real transportation system.

The research contents are as follows: Section 2 reviews the literature and shows points to be further optimized. Section 3 proposes the optimized modeling method for a CNet. Section 4 introduces the data of the case study and the research method of robustness. Section 5 analyzes the statistical characteristics of five networks in Jiangsu. Section 6 compares the robustness of five networks in Jiangsu. Section 7 explores the robustness of CNets modeled by our method and previous methods. Section 8 summarizes the research conclusions and proposes some suggestions.

2. Literature review

2.1. Modeling method for the transportation network

To theoretically analyze the characteristics of a transportation network, the first step is to mathematically depict the real network. In previous research, the network's topology was often represented using a graph. Let us consider an unweighted and undirected network $G=(V,E)$, where G represents the analyzed network, V is the nonempty set of vertices and E is the set of edges. The relationship between V and E can be represented as $E \in V \times V$ indicating that the set of edges is a subset of the connections between any two points. This mathematical representation applies to various types of networks such as power networks, the Internet [2], interpersonal networks and transportation networks [3].

The process of abstracting objects from a real network into vertices and edges in a graph can be addressed using the concept of modeling space, as proposed by Von Ferber et al [4]. The modeling space encompasses four methods: space L, space C, space P and space B [5,6]. In the analysis conducted by Lin et al., the evolution process of urban public transportation networks at different times was examined, highlighting the distinct topological characteristics between networks constructed using space L and space P [7]. Kurant et al. observed differences in the statistical properties of networks modeled under various methods such as space L, space P and space C using the Swiss railway network [8]. Porta et al. discovered that the highway network modeled under space L lacked the scale-free property, whereas the network modeled under space C exhibited scale-free characteristics [9]. These findings indicate that the properties of a network can differ based on the chosen modeling space.

Moreover, the selection of vertices and edges varies depending on the spatial scale considered. For instance, Dau S. H. et al. employed intersection conflict points and vehicle trajectory lines [10], while Wang [11] and Li [12] focused on airports and airline routes. Boasa P.R.V. et al., on the other hand, utilized cities and highway sections [13]. Hence, when studying regional transportation, it is crucial to select appropriate objects based on the spatial scale under investigation.

2.2. Research contents of the multimodal transportation network

Transportation networks can be categorized as single-mode or multimodal networks. Single-mode networks encompass various research objects, including urban transit networks [14,15], urban road networks [16,17], railway operation networks [18,19] and aviation operation networks [20,21]. For instance, Zhang examined high-speed railway networks in China, the U.S. and Japan, comparing their statistical characteristics using metrics such as average degree, maximum degree and average medium [22]. Sen investigated the railway network in India and discovered its small-world property [23]. Bagler G reviewed the aviation operation network in India and identified it as a small-world network characterized by a truncated power-law degree distribution [24]. Sienkiewicz J. et al. studied bus networks in 22 cities in Poland, summarized the degree distribution patterns and found that all of them exhibited small-world properties [25].

In the case of multimodal networks, the research primarily focuses on connecting different networks. Two main approaches are commonly used to construct multimodal networks.

1) Supernetwork: The supernetwork is a multilayer complex network model that characterizes the composition of multimodal networks. It connects various layers of different modality sub-networks, primarily through virtual arc segments, forming a nested multilayer network model where

each layer can interconnect with one another [26–28].

This method finds extensive application in the construction of urban transportation networks. For example, Xu constructed a multimodal supernetwork model among cities and proposed a stochastic equilibrium allocation method for intercity transportation systems [29]. Ding depicted the entire process of residents' public transit travel through a supernetwork, considering components such as line transfers and residents' walking access to bus stops [30]. Lozano established a general bus-subway composite supernetwork, designed a path search algorithm and examined users' path preference selection in urban public transportation [31].

The supernetwork approach has also been successfully applied to the study of regional comprehensive transportation systems. Shi constructed an airway-railway intermodal network using a supernetwork and conducted an in-depth analysis of road sections and node impedance functions within this composite network [32]. Deng, on the other hand, developed a three-layer supernetwork of highways, railways and waterways for freight planning and forecasting in the Yangtze River Economic Belt [33]. Xu applied the supernetwork approach in the integration of regional comprehensive transportation logistics, encompassing infrastructure, information resources and organizational networks [34].

2) Merging different networks: This approach involves merging nodes and routes from different networks to achieve the fusion of multiple modes. For instance, Luo combined bus stops and subway stops at the same location into a single node in the study of a composite urban bus-subway transit network [35]. Xu et al. merged nodes that spatially correlated roads and railways when studying the railway-aviation composite network [36]. Feng et al. treated railway stations and airports as homogeneous vertices and established edges representing transfer routes [37]. Ouyang treated railway stations and airports within the same city as a single point [38]. Luo et al. combined a subway station and a bus station with close distances into one vertex when studying conventional buses and subways and represented the bus line and subway line passing through the same two vertices as one edge [39]. Li regarded three adjacent subway stations and four bus stations as a unit and connected each station in the unit to represent the transfer section [40]. Liu utilized a weighted bipartite graph to construct the transfer network inside the station [41].

2.3. Robustness analysis of the transportation network

Studies on the robustness of transportation networks can be categorized into two main categories: topology-based robustness and operational robustness.

Topology-based robustness analyzes unweighted topological networks to identify highly influential nodes. Classic indicators used to evaluate node importance include degree centrality [42], betweenness centrality, and closeness centrality [43]. Demšar et al. proposed a mathematical method that utilizes degree centrality and clustering coefficient to identify critical locations in street networks [44]. Chen employed topological indices such as average degree, relative maximum connectivity graph and efficiency to analyze urban transport networks in Beijing and developed a new indicator combining node degree and betweenness to better reflect network resilience [45]. Duan and Lu conducted an empirical study on six city road networks using betweenness centrality to analyze robustness and identify critical points [46].

Additionally, researchers have developed new indicators such as collective influence (CI), which measures node importance by aggregating degrees over all neighbors within a given radius [47] and CoreHD, a method that removes the highest degree node in 2-core networks first, followed by tree-breaking [48].

Operational robustness focuses on analyzing weighted networks where weights represent flows, congestion or capacities. Cats et al. integrated capacity degradation results per edge into network robustness assessment using Amsterdam's urban public transport network as a case study [49]. Shang proposed a novel indicator called relative area index (RAI) based on traffic assignment theory to reveal the robustness of multi-scale urban road networks, which outperformed traditional topological metrics like weighted betweenness centrality when facing global disruptions [50]. Ouyang et al. introduced mathematical models and solution algorithms to identify optimal robustness-based and resilience-based protection strategies for critical infrastructure systems [51]. Kermanshah and Derrible developed a geographical and multi-criteria vulnerability assessment method to quantify the impacts of extreme earthquakes on road networks using Los Angeles and San Francisco as case studies [52].

Some researchers have combined both topology-based and operational perspectives to systematically investigate the resilience characteristics of networks under static and dynamic conditions. They construct frameworks for network robustness analysis that capture the relationship between topological and operational indices. For example, Shang applied topological and operational indices to analyze urban road networks and assess their robustness against local disruptions [53]. Liu proposed a resilience assessment framework considering network function, structure and recovery performance under different attacks to optimize urban road networks [54]. Zhang applied static metrics such as node degree, betweenness and closeness, as well as dynamic metrics like flow degree to analyze the robustness of the directed weighted urban railway network in Hong Kong under cascading failures [55].

When simulating network failure, researchers commonly employ random and calculated attack methods [56]. Random attacks simulate natural disasters, while calculated attacks simulate intentional human damage. Building on classic methods, researchers have proposed new attack strategies. For example, Li et al. improved spatially localized failure models to simulate failure caused by typhoons, where nodes and edges are affected within a specific circular area [57].

2.4. Summary of the literature

To summarize, although researchers have made significant progress in studying transportation network robustness, there are several areas that still require further optimization and exploration.

Lack of unified modeling rules for multimodal CNet: Existing studies predominantly focus on single-mode or composite networks, lacking analysis of CNet that include highways, railways, waterways and aviation. Additionally, there is a lack of standardized mapping rules for vertices and edges, failing to fully represent the mode transfer process facilitated by transit hubs.

Insufficient statistical characteristics and robustness analysis of multimodal CNet: Previous research primarily concentrates on single-mode or two-mode composite networks. These studies have revealed scale-free and small-world characteristics in bus, subway and aviation networks. However, there is limited research on the topological structure and robustness characteristics of CNet. What is the performance of a comprehensive transportation network in terms of the degree distribution, scale-free characteristics and the small-world? How does the robustness of multi-modal CNet change under various attacks? Are there any differences between the robustness of CNet and the single-mode network? What common trends can be observed in their robustness variations? These questions remain unanswered.

Insufficient comparative analysis of CNet robustness under different transfer conditions: Different transfer conditions in CNet can be represented by various modeling methods. Previous

studies often oversimplify the transfer process and neglect the detailed design of transfer points between different modes. Can this simplification method accurately assess the robustness of CNet? Can the detailed mode transfer design improve the robustness of CNet? How much can this kind of design affect the network's robustness? These questions remain unanswered.

3. Network modeling method

3.1. Overall network structure

CNet includes four kinds of single-mode networks and the micronetwork of transit hubs. Single-mode networks refer to the highway, railway, navigation channel and airway transportation networks (HNet, RNet, NNet and ANet, respectively). The micronetwork of transit hubs includes the transfer network inside the hub and the connecting section outside the hub. The transit hub point (THP) is defined as the vertex with a mode transfer function, which includes the vertices of railway stations, harbors and airports. Figure 1 shows the network structure of CNet.

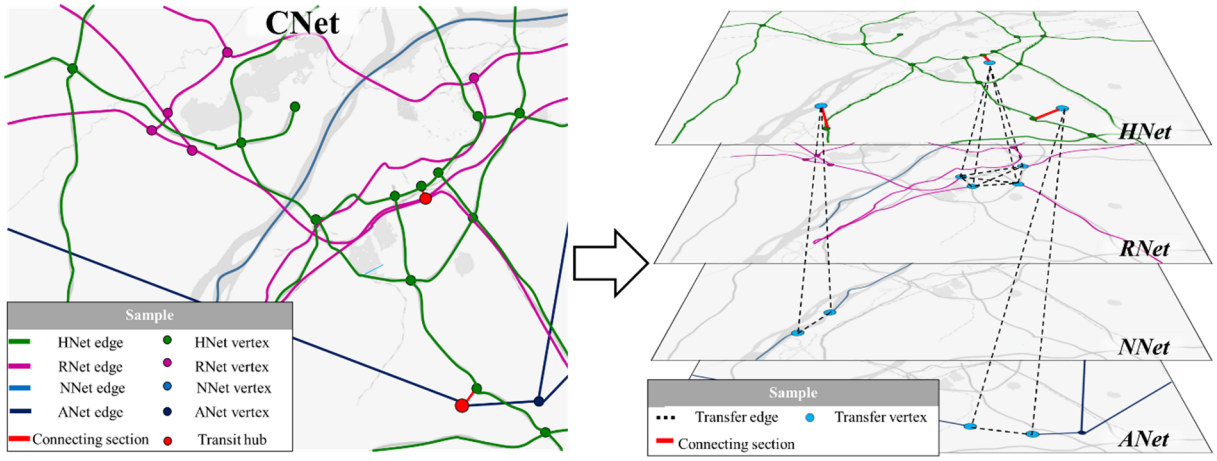

Figure 1. The structure of CNet.

CNet can be described as $G_C = (V_C, E_C)$, where V_C and E_C refer to the vertices and edges in CNet. Similarly, HNet, RNet, NNet and ANet can be described as $G_H = (V_H, E_H)$, $G_R = (V_R, E_R)$, $G_N = (V_N, E_N)$ and $G_A = (V_A, E_A)$, respectively. The construction method of the above network will be explained in detail in Section 3.3.

The set of the THP is defined as V_{THP} and a THP in the set is denoted by v_{THP}^k, where $k = 1, 2, ..., |V_{THP}|$. The construction method of the connecting section will be explained in detail in Section 3.2. A connecting section is denoted as $e_{P_1P_2}^k$. The set of all such connecting sections in the CNet is denoted as $E_{connect}$. The construction method of the mode transfer network of the THP k will be explained in detail in Section 3.2. The mathematical expression is $G_J^k = (V_J^k, E_J^k)$, where V_J^k denotes the set of transfer vertices and E_J^k denotes the set of transfer edges.

Thus, the mathematical expression of CNet is shown in Eq (1).

$$G_C = (V_C, E_C)$$
$$\begin{cases} V_C = V_H \cup V_R \cup V_N \cup V_A \cup V_J^1 \cup V_J^2 \cup ... \cup V_J^k - V_{THP} \\ E_C = E_H \cup E_R \cup E_N \cup E_A \cup E_{connect} \cup E_J^1 \cup E_J^2 \cup ... \cup E_J^k - (E_{THP}^1 \cup E_{THP}^2 \cup ... E_{THP}^k) \end{cases} \tag{1}$$

3.2. Modeling method for the transit hub

3.2.1. Transfer connection inside the hub

The transfer connection inside the hub connects all the roads connected by the hub in pairs. It depicts the transfer process from one road to another. Define the transfer network in v_{THP}^k as $G_J^k = (V_J^k, E_J^k)$. The modeling progress can be divided into three steps.

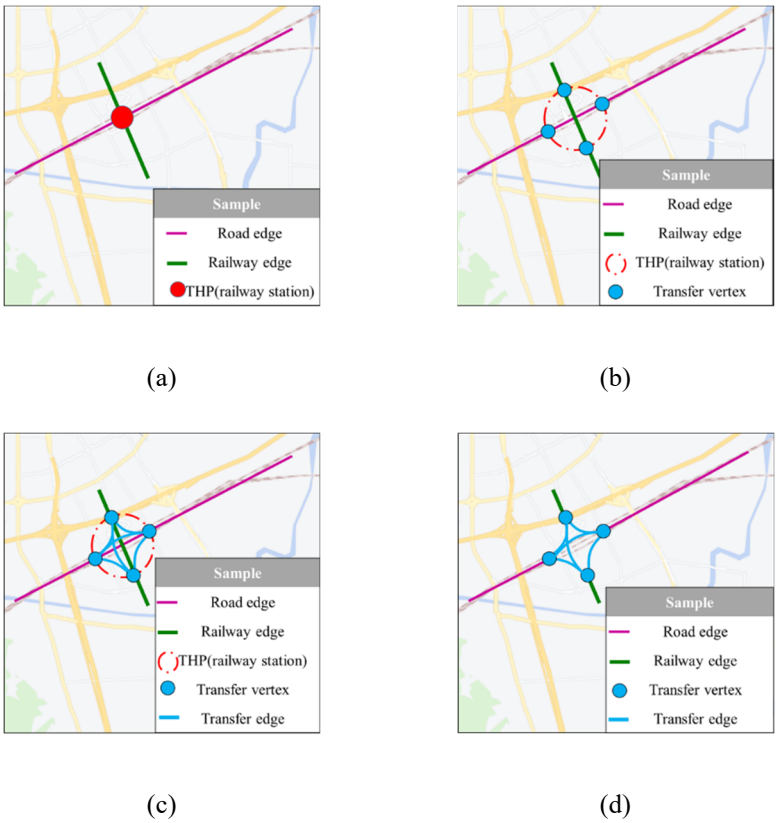

Figure 2. The construction process of the mode transfer network.

Step 1: Adding the transfer vertex. Make a circle with a radius of 1 (1 unit after standardization according to the spatial scale). The intersections between the circle and all n edges connecting with v_{THP}^k are the newly added transfer vertices, denoted as $v_J^{k,1}, v_J^{k,2}, ... v_J^{k,n}$. They are represented as blue dots in Figure 2(b). The set of all freshly added transfer vertices in v_{THP}^k is defined as V_J^k.

Step 2: Adding the transfer edge. Generate C_n^2 edges among n transfer vertices as transfer edges. Each edge is denoted as $e_J^{k,ij}$, where $i, j \in V_J^k$ and $i \neq j$. Transfer edges are represented as blue lines in Figure 2(c). The set of all freshly added transfer edges in v_{THP}^k is defined as E_J^k.

Step 3: Deleting THP. Delete v_{THP}^{k} (represented as the red dashed circle in Figure 2(c)) from all sets, including V_{THP}, V_H, V_R, V_W and V_A. Then, delete the edges between v_{THP}^{k} and $v_J^{k,1}, v_J^{k,2}, \ldots v_J^{k,n}$ (represented as green and purple solid lines surrounded by the red dashed circle in Figure 2(c)) and define the set of all these kinds of edges as E_{THP}^{k}, as shown in Figure 2(d).

The number of vertices N_{vertex} and edges L_{edge} in G_J^k is shown in Eqs (2)–(4).

$$N_{vertex} = \sum_{i=1}^{4}(x_i - 2) + M \tag{2}$$

$$L_{edge} = \frac{1}{2}[\sum_{i=1}^{4}(x_i - 2) + 2M][(\sum_{i=1}^{4}(x_i - 2) + 2M - 1)] \tag{3}$$

$$n = \sum_{i=1}^{4} x_i \tag{4}$$

where M is denoted as the number of traffic modes connected by v_{THP}^{k} $(1 \le M \le 4)$. x_i is denoted as the edge number of the mode i $(x_i \ge 2)$ and the i value ranges from 1 to 4, indicating highway, railway, navigation channel and airway. n is denoted as the total number of edges connected with v_{THP}^{k}.

3.2.2. Transfer connection outside the hub

The transfer connection inside the hub refers to the edge connecting the hub and the outside highway, as shown by the red edge in Figure 3. The connection is meant to solve an important problem. In the real world, when the hub is located inside the city there is much slow traffic around it so the links connected to it tend to be low-grade roads. When modeling, if only six types of highways are reserved, the hub will not be connected to the HNet. Therefore, we add an edge between the hub and the external road vertex as an abstract representation of the low-grade road. Figure 3 shows HNet vertex $v_{hw}^{1} \in V_H$, HNet edge $e_{cw}^{1}, e_{cw}^{2} \in E_H$, THP $v_{THP}^{k} \in V_{THP}$ and THP $v_{THP}^{k} \in V_R$. RNet $e_{rw}^{1}, e_{rw}^{2}, e_{rw}^{3}, e_{rw}^{4} \in E_R$. Define $e_{P_1P_2}^{k}$ as the connecting section, where $P_1 = v_{hw}^{1}, P_2 = v_{THP}^{k}$.

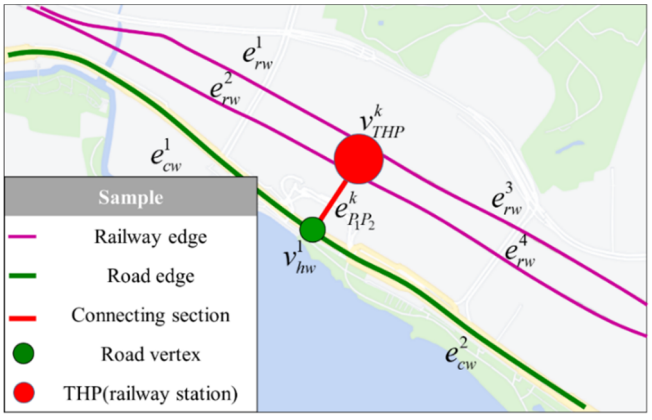

Figure 3. The model of the connecting section between the hub and the external highway.

3.2.3. Transfer connection of the expressway

There is another kind of special hub, which is the expressway entrance and exit (EEE). It connects the expressway and the other roads. Since most expressways in China are tolled, the EEE usually consists of ramps, toll stations, checkpoints, etc., as shown in Figure 4(a). An optimized method is proposed to represent the topology structure of the EEE, as shown in Figure 4(b). Three vertices and two edges are used. $v_{hw-ring}$, v_{toll} and $v_{ring-cw}$ represent the intersection formed by the ramp and expressway, toll stations or checkpoints and the intersection formed by the ramp and the other road, respectively. e_{ring}^{up} and e_{ring}^{down} represent two kinds of ramps. In this model, if simulating the EEE failure caused by bad weather, traffic congestion, traffic control, etc., only v_{toll} needs to be removed. It will not affect the connectivity of the expressway, which is consistent with reality.

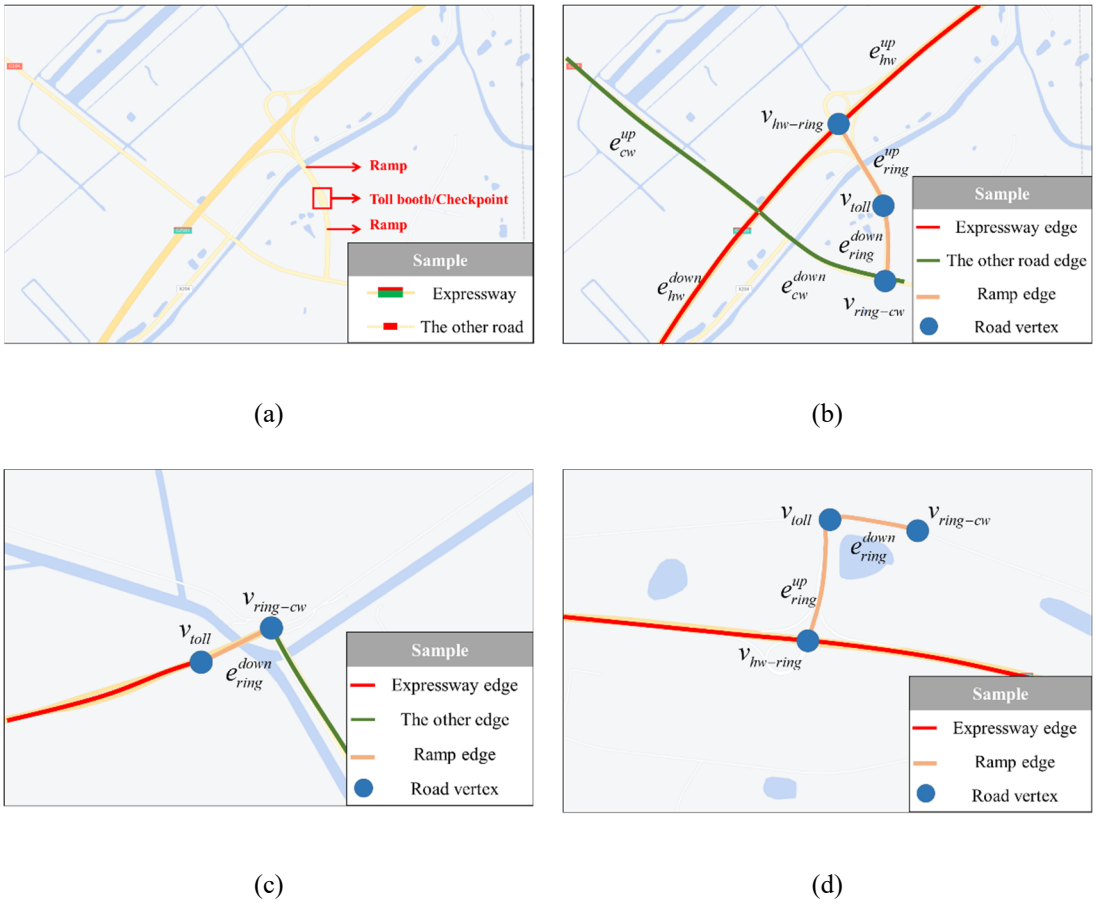

(a) (b)

(c) (d)

Figure 4. Modeling method for EEE.

In addition, two special cases must be discussed. First, for the starting and ending points of the expressway, only v_{toll}, $v_{ring-cw}$ and e_{ring}^{down} need to be retained, as shown in Figure 4(c). Second, when the road connected with the expressway does not belong to the six kinds of highways in HNet, $v_{hw-ring}$, v_{toll}, $v_{ring-cw}$, e_{ring}^{up} and e_{ring}^{down} is still used but $v_{ring-cw}$ is only connected to e_{ring}^{down} and no other edges are connected, as shown in Figure 4(d).

3.3. Modeling method for a single-mode network

The core of the modeling method for a single-mode network is to clarify the mapping rules, which refer to the correspondence between existing traffic elements and the abstract network. There are three steps.

Step 1: Specify the modeling object. Regional transportation gives more attention to trunk channels. Therefore, it is necessary to clarify the selection criteria of each element in the real network.

Step 2: Specify the meaning of vertices and edges. Traffic elements represented by the vertices and edges differ in different situations. Whatever they represent must be clarified at the same spatial scale.

Step 3: Addressing some special situations. Some exceptional cases need to be discussed to more appropriately reflect the topological relationship of the real.

Table 1. The Establishment of Mapping Rules.

	Step 1	**Step 2**		**Step 3**
		V^*	E^*	
HNet	National expressways, provincial expressways, national trunk highways, provincial trunk highways, urban expressways and urban main roads.	Plane intersections, stereo intersections, expressway entrances and exits and toll stations	The main highway sections existing between two vertices	(i) V_H excludes intersections formed by roads other than six modeling objects. (ii) E_H only includes the main road of the highway section
RNet	The national high-speed railway, the national heavy haul railway, and the national railway Grade I-III	The railway stations and the large overpasses intersected by two or more railway lines.	The main railway sections.	All lines should be reserved when a railway station is connected with multiple lines.
NNet	The navigation channel Grade I, II, III	Wharves, locks in the inland waterway, and intersections of inland waterways.	Navigation channel sections.	The intersection of the marine channel is not considered
ANet	Airway, not airlines.	Airports, reporting points, VOR, DME and NDB**.	The airway sections.	When the positions of different types of vertices coincide, only one needs to be reserved.

*V and E separately represents the vertex and the edge of the single-mode network.

**VOR, DME and NDB are the abbreviations of nodes with definite functions on the airway. VOR: very high frequency omnidirectional range. DEM: distance measuring equipment. NDB: nondirectional beacon.

In **Step 1**, when constructing HNet, inter-city connectivity and transit traffic requirements are mainly considered. In addition, the administrative grade of a highway can better reflect its function in the network than the technical grade. Therefore, these six paths are chosen as model objects. When constructing ANet, the airway refers to the route that an aircraft needs to follow when flying in the airspace, but the airline is a line operated by the airline company. From the perspective of the infrastructure network, the airway is similar to the highway, railway and navigation channel. Therefore, it is chosen as modeling the object instead of the airline.

4. Case study and robustness analysis method

4.1. Data overview of the case

The case object is a comprehensive transportation network in Jiangsu Province, a typical coastal province in China. The highway, railway and navigation data are derived from the electronic navigation map data provided by NavInfo [58]. The aviation data are derived from the enroute chart (Revision 15) published by the Civil Aviation Administration of China (CAAC) in June 2021 [59].

Table 2. Comprehensive transportation network data of Jiangsu Province.

	Mode	Original data	Filtered data
Number of nodes	Highway	136,881	39,007
	Railway	10,650	3046
	Navigation channel	9084	2521
	Airway	164	69
	Other	79,928	0
	Sum	236,707	44,643
Number of sections	Highway	269,151	77,669
	Railway	16,835	4859
	Navigation channel	13,510	3898
	Airway	326	118
	Other	27,286	0
	Sum	327,108	86,544

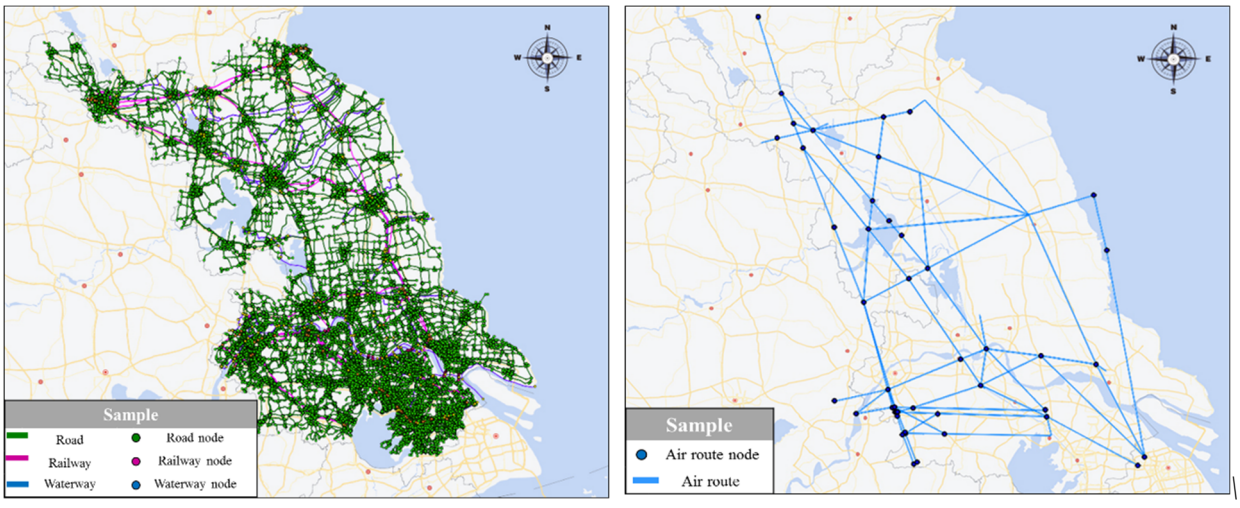

(a) Spatial distribution of the navigation map data (b) Spatial distribution of the CAAC enroute chart

Figure 5. Spatial distribution of data for Jiangsu Province.

The electronic navigation map data contain traffic nodes, sections, points of interest (POIs) and sidewalk sections. Therefore, the data are extensive. According to Section 3.3, the original data were

filtered and the amount of data decreased significantly. Table 2 shows the number of nodes and sections. Both the node and section numbers of the highway are the largest. The data spatial distribution is shown in Figure 5.

4.2. Evaluation index for robustness

4.2.1. Change in global efficiency $\eta(E(G))$

Global efficiency is to explore the connectivity condition of the connected or disconnected network and its formulation is written as follows:

$$E(G) = \frac{1}{N(N-1)} \sum_{i \neq j \in G} \frac{1}{d_{ij}} \tag{5}$$

d_{ij} represents the distances between any two vertices and N is denoted as the vertex number, where G is the network. If the non-weighted network is completely connected, $E(G) = 1$. When the network is continuously attacked and isolated vertices appear, the distance between vertices will continue to increase, so $E(G)$ decreases. According to Eq (5), the change in global efficiency can be calculated as:

$$\eta(E(G)_T) = \frac{E(G)_T - \min\{E(G)_T\}}{\max\{E(G)_T\} - \min\{E(G)_T\}} \tag{6}$$

$E(G)_T$ represents the global efficiency when T vertices are attacked, where $T = 1,2,...,N$. $\max\{E(G)_T\}$ represents the maximal value of the global efficiency during the entire progress of the attack and $\min\{E(G)_T\}$ represents the minimal one. $\eta(E(G))$ is a normalized index, that is $0 \leq \eta(E(G)) \leq 1$.

4.2.2. Change in maximal connected subgraph $\eta(R(G))$

The maximal connected subgraph is to measure the completeness of the network. The change of it can be calculated as follows:

$$\eta(R(G)) = \frac{N(MCG)_T - \min\{N(MCG)_T\}}{N(G) - \min\{N(MCG)_T\}} \tag{7}$$

$N(MCG)_T$ represents the vertex number of the maximal connected subgraph when T vertices are attacked, where $T = 1,2,...,N$. $N(G)$ represents the vertex number of G. The meaning of $\min\{\}$ is as same as that above. The index is normalized, that is $0 \leq \eta(R(G)) \leq 1$. A higher $\eta(R(G))$ means the network can maintain a good connection, which also means the graph is more robust.

4.2.3. Change in standard structural entropy $\eta(H(G))$

Structural entropy is to explore the uniformity of the network and formulation is written as follows:

$$H = -\sum_{i=1}^{N} I_i \ln I_i \tag{8}$$

$$I_i = \frac{k_i}{\sum_{j=1}^{N} k_j} \tag{9}$$

H represents the structural entropy of the network. I_i is the importance of vertex i. To eliminate the influence of vertex numbers, H need to be normalized as follows:

$$H_{\max} = \ln N \tag{10}$$

$$H_{\min} = \ln[4(N-1)]/2 \tag{11}$$

$$H(G) = \frac{H - H_{\min}}{H_{\max} - H_{\min}} = \frac{-2\sum_{i=1}^{N_i} I_i - \ln[4(N-1)]}{2\ln N - \ln[4(N-1)]} \tag{12}$$

$H_{\max}$ is the maximal value of the structural entropy when the degree values of all vertices are the same. $H_{\min}$ is the minimal value, when all vertices connect with a special vertex. According to Eq (12), the change of the standard structural entropy can be calculated as:

$$\eta(H(G)_T) = \frac{H(G)_T - \min\{H(G)_T\}}{\max\{H(G)_T\} - \min\{H(G)_T\}} \tag{13}$$

$H(G)_T$ represents the standard structural entropy when T vertices are attacked, where $T = 1, 2, ..., N$. The meaning of $\max\{\}$ and $\min\{\}$ is as same as those above. $\eta(E(G))$ is a normalized index, that is $0 \le \eta(E(G)) \le 1$. If $\eta(E(G))$ maintains steadily under attack, the network is more robust.

4.2.4. Robustness composite indicator V

The robustness composite indicator is to evaluate the robustness of the network from multiple dimensions, including connectivity, completeness and uniformity. The formulation is written as follows:

$$V = \lambda_1 \times \eta(E(G)) + \lambda_2 \times \eta(R(G)) + \lambda_3 \times \eta(H(G)) \tag{14}$$

λ_1, λ_2 and λ_3 is denoted as the weight of $\eta(E(G))$, $\eta(R(G))$ and $\eta(H(G))$, respectively. They indicate the importance of connectivity, completeness and uniformity in the network. $\lambda_1, \lambda_2, \lambda_3 \in (0,1)$ and $\lambda_1 + \lambda_2 + \lambda_3 = 1$. $0 \le V \le 1$. The larger the value of V, the more robust the network. In this article, $\lambda_1 = \lambda_2 = \lambda_3 = 1/3$.

4.2.5. Critical ratio of network failure CR

The critical ratio of network failure is to show when the network fails completely and the formulation is written as follows:

$$CR = \frac{CP}{N(G)} \times 100\% \tag{15}$$

$$CP = \varphi(V = \frac{1}{100} V^0) \tag{16}$$

CP is denoted as the critical point of network failure, which is the number of vertices that have been attacked when V is less than 1% of the initial value V^0. CR is normalized, that is $0 \le CR \le 1$. The larger the value of CR, the more robust the network.

4.3. Experimental scheme for robustness

This paper proposes four attack strategies. The random attack (RA) is randomly selecting an attacked vertex without considering the difference and all vertices have the same probability of being selected. A calculated attack is a purposeful attack based on the importance of vertices. However, there are a large number of vertices with the same degree value. To clarify the attack sequence of these vertices we formulate three different calculated attack strategies, which are regular calculated attack (CAR), calculated attack considering update degree (CAUD) and calculated attack considering random selection (CARS). The steps of the four attack strategies are shown in Figure 6.

5. Statistical characteristics of the network

5.1. Degree distribution

From Figure 7, it can be seen that the degree of the five networks is mainly concentrated between 1 and 4, and there are few vertices with high degrees. Among them, the curves of HNet and CNet are relatively close. The degree is concentrated between 2 and 4 (94.4 and 88.7%, respectively) and the high degree ($k > 4$) is less (0.2 and 3.7%, respectively). Although the degrees of RNet and ANet are concentrated between 1 and 3 (86.3 and 69.0%, respectively), ANet has more high-degree vertices (15.5%), but RNet has fewer (2.0%). The distribution of the NNet degree is relatively narrow, ranging from 1 to 4, mainly concentrated between 2 and 3 (79.1%).

Why are there many vertices with a degree value of 3 in HNet? There are three reasons: First, each EEE contributes 1 or 2 vertices with a degree of 3. There are 447 EEEs in HNet, so 671 vertices with a degree value of 3 are contributed. Second, these vertices are primarily intersections of expressways, national or provincial trunk highways and urban roads. This reflects the apparent hierarchical phenomenon of HNet: a small number of expressways and national trunk highways serve a large area and a large number of provincial trunk highways and urban roads serve a small area. This phenomenon is more evident at the city boundary, as shown in Figure 8(a). The intersection vertices are highlighted. Third, Jiangsu is a coastal province and acts as a natural barrier and many east-west highways terminate in north-south coastal highways. Figure 8(b) shows the road in the coastal city of Yancheng. In addition, there are some large natural lakes such as Taihu Lake, Hongze Lake, Gaoyou Lake, Shaobo Lake and Luoma Lake. The highway ends at the road encircling the lake. Figure 8(c) shows the road around Hongze Lake. This kind of vertex is highlighted.

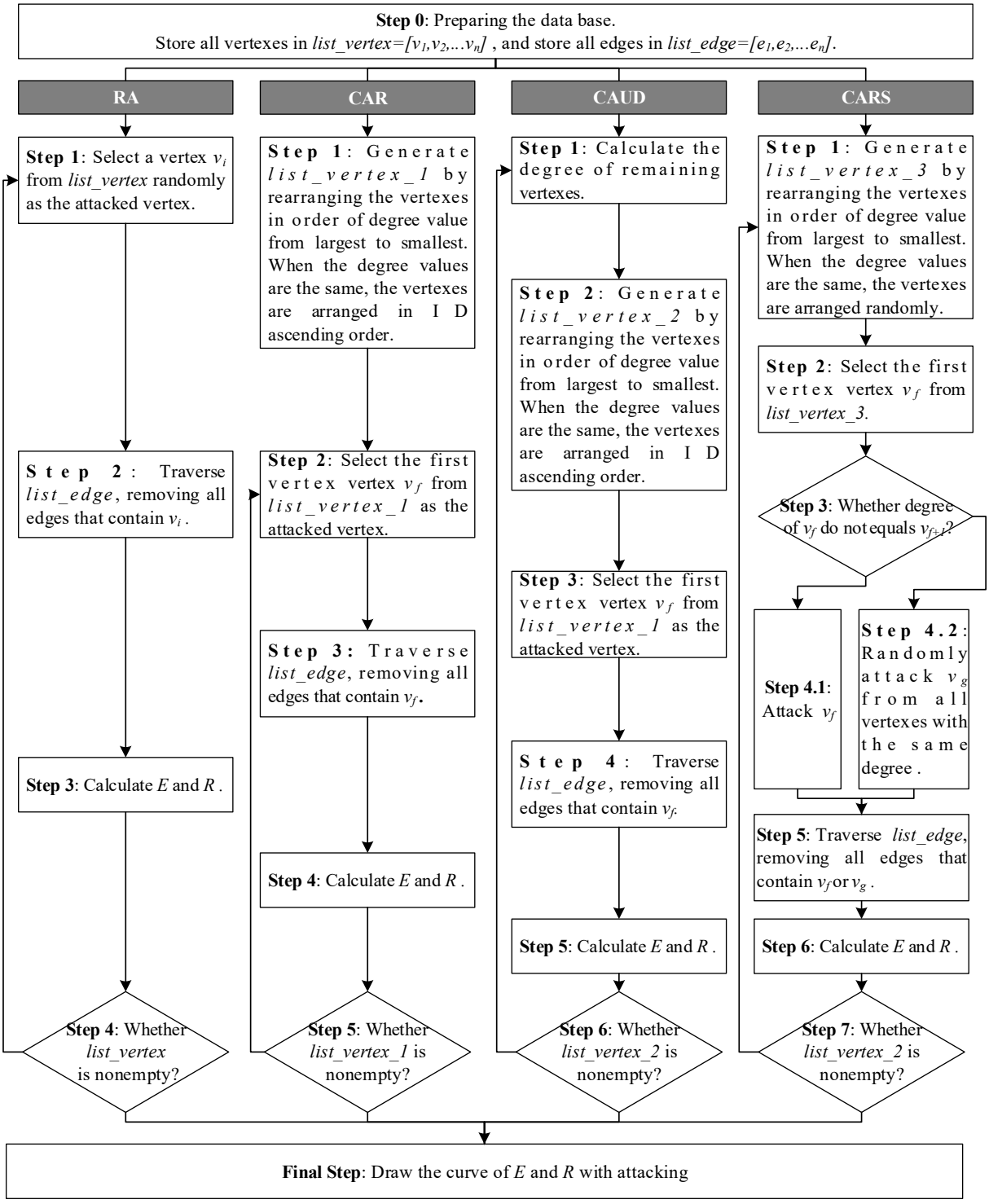

Figure 6. Steps of the four attack strategies.

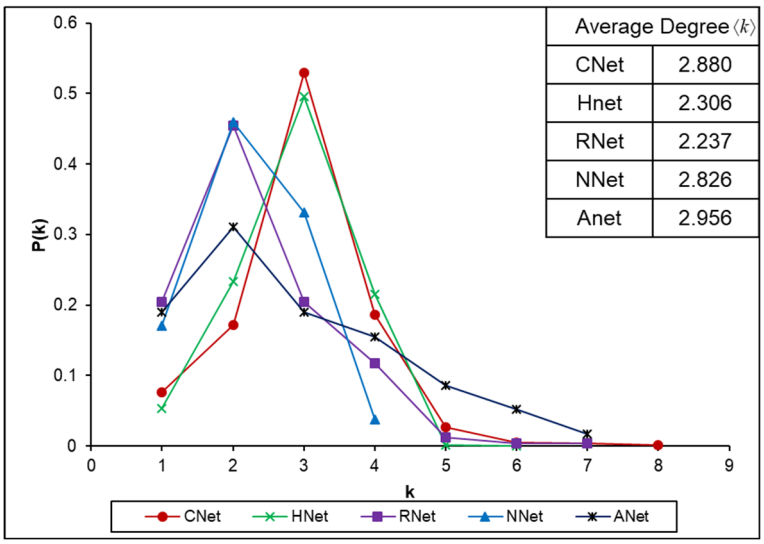

Figure 7. Degree distribution curve.

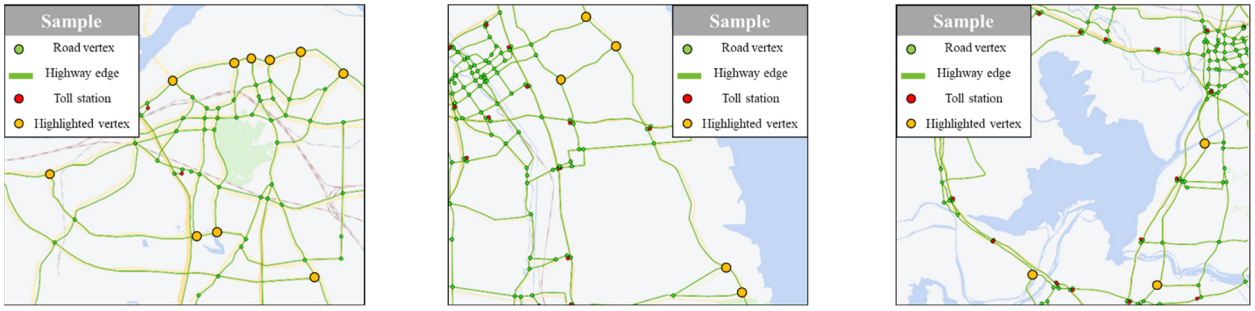

(a) (b) (c)

Figure 8. The reason for forming the vertices with a degree value of 3.

5.2. Scale-free and small-world

To analyze the scale-free property of the networks, their degree distribution curves are fitted in the double logarithmic coordinate system by a power-law distribution function. Barabasi noted that the network is scale-free when the function's slope is $2 < \gamma < 3$. The network has the characteristics of both a random and scale-free network when $\gamma > 3$. As shown in Table 3, HNet, RNet, NNet and CNet are not scale-free networks, but ANet is.

Furthermore, the Poisson distribution is applied to fit the degree distribution curves of the five networks to explore whether they belong to random networks. As shown in Table 3, the fitting indices are not significant. It shows that none of the five networks is a random network.

Finally, two indicators are calculated to explore the small-world property. Barabasi also noted that when $\langle d \rangle \approx \frac{\ln N}{\ln \langle k \rangle}$, the network is small-world. As shown in Table 3, only ANet has the small-world property, while the other four networks do not.

Table 3. Indicators of the network statistics feature.

Property	Indicator	HNet	RNet	NNet	ANet	CNet
Random network	Poisson R^2	0.0272	0.1513	0.0136	0.0666	0.0872
	Poisson $P>\|z\|$	0.720	0.440	0.815	0.583	0.523
	Poisson Log likelihood	-2.389	-2.192	-2.027	-2.351	-2.503
Scale-free	Power-law γ	-5.87	-4.29	-3.42	-2.07	-3.98
Small-world	$\frac{\ln N}{\ln\langle k\rangle}$	7.649	6.632	3.586	3.586	7.710
	$\langle d\rangle$	26.98	12.478	4.205	4.205	22.58
	Small-world or not?	NO	NO	NO	YES	NO

Why is the judgment of the scale-free property of NNet different from that of predecessors such as Li [60] and Lou [61]? This can be explained by different modeling objects and mapping rules. The modeling object in Li's research is the shipping route network near ports. Ships here are subject to dispatch rather than free navigation. When the network is scale-free, many routes are connected to a few points, which is conducive to dispatching. In Luo's research, the vertex represents the intersection of waterways or an administrative boundary. However, in this paper, waterway intersections, harbors and locks are considered. Especially with the addition of locks, many vertices with a degree value of two are added. Similarly, because of the different modeling objects and mapping rules, the small-world property of NNet is also different from predecessors. However, the conclusions of HNet, RNet and ANet are consistent with the research results of Fu [62], Zhao [63] and Bagler G [24].

5.3. Network spatial scale

From the number of vertices and edges, it can be seen that HNet occupies the primary position in CNet. In addition, there are other findings: (i) Compared with HNet, $d_{\max}$ of CNet is smaller. (ii) Compared with HNet, $\langle d\rangle$ of CNet is smaller. (iii) Compared with HNet, $\langle C\rangle$ of CNet is larger.

Table 4. Statistical characteristics.

Network	N	L	$d_{\max}$	$\langle d\rangle$	$\langle C\rangle$
HNet	3265	4701	76	26.98	0.033
RNet	255	294	37	15.220	0.089
NNet	211	236	31	12.478	0.014
ANet	58	90	10	4.205	0.151
CNet	4257	6291	55	22.58	0.085

There are two reasons for the difference in $\langle d\rangle$. On the one hand, the railway, navigation channel and airway connect more vertices. On the other hand, RNet, NNet and ANet result in an average effect due to the smaller number of vertices and shorter average path length.

Similarly, there are two reasons for the difference in $\langle C\rangle$. On the one hand, considering the transfer network, THP enables the surrounding vertices to communicate with each other more tightly, thus generating more accessible paths and increasing the agglomeration degree. On the other hand, $\langle C\rangle$ of RNet, NNet and ANet is higher than that of HNet, so the clustering degree of CNet is increased after integration.

6. Robustness analysis for the single-mode network and CNet

6.1. Robustness analysis for the single-mode network

Under different attack strategies, four networks exhibit varying levels of robustness. They demonstrate greater robustness under RA and CAR, but their robustness is significantly lower under CAUD and CARS. Figure 9 illustrates that regardless of the attack strategy used, the curves of V for CAUD and CARS consistently remain lower than those for RA and CAR throughout the attack. This indicates that the connectivity, completeness and uniformity of the networks are more severely affected under CAUD and CARS compared to RA and CAR even when an equal number of vertices are attacked. Similar patterns are observed for other indices as well.

The values of CR under different attack strategies confirm the same robustness trend. In HNet, the CR values under RA, CAR, CAUD and CARS are 94.64, 92.37, 55.90 and 56.36%, respectively. In ANet, CR are 89.66, 79.31, 46.55 and 51.72%, respectively. CR under RA and CAR is consistently higher than that under CAUD and CARS, indicating that the network can withstand more severe attacks before experiencing failure.

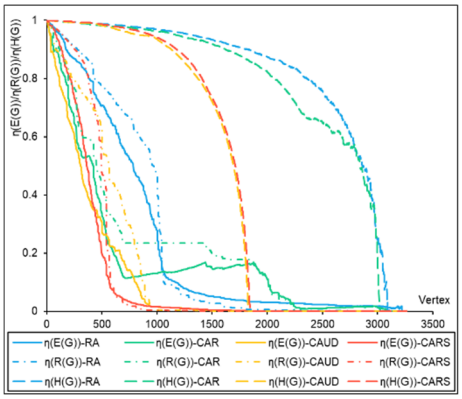

(a) HNet $\eta(E(G))/\eta(R(G))/\eta(H(G))$

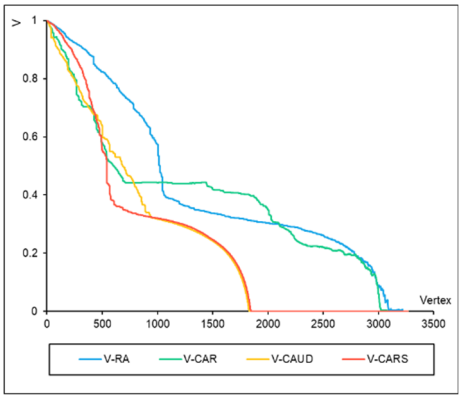

(b) HNet V

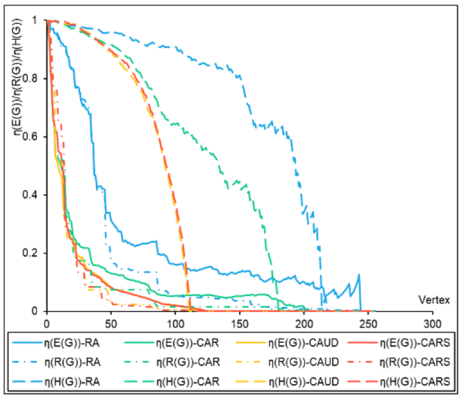

(c) RNet $\eta(E(G))/\eta(R(G))/\eta(H(G))$

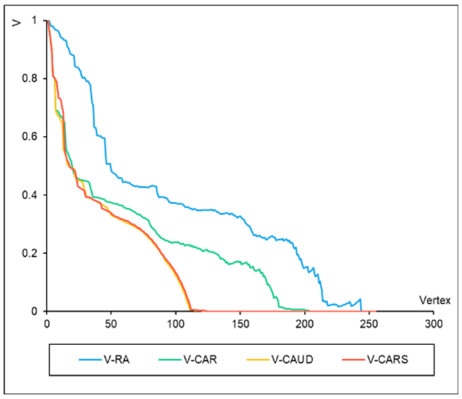

(d) RNet V

Continued on next page

Figure 9. The robustness results of the single-mode network.

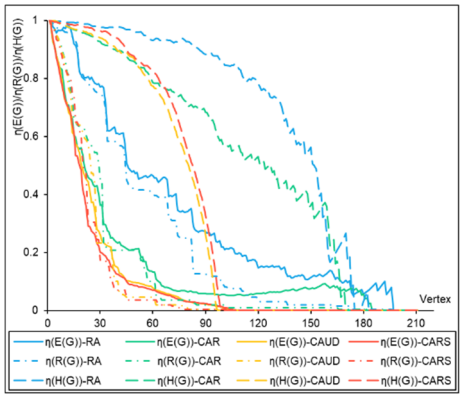

(e) NNet $\eta(E(G))/\eta(R(G))/\eta(H(G))$

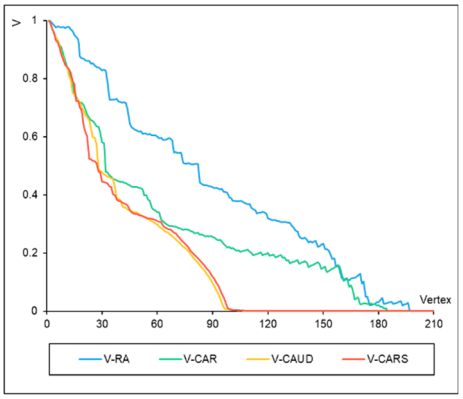

(f) NNet V

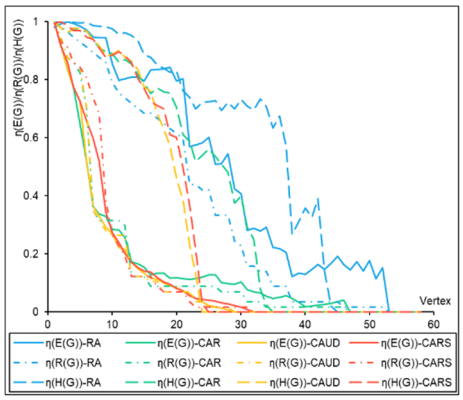

(g) ANet $\eta(E(G))/\eta(R(G))/\eta(H(G))$

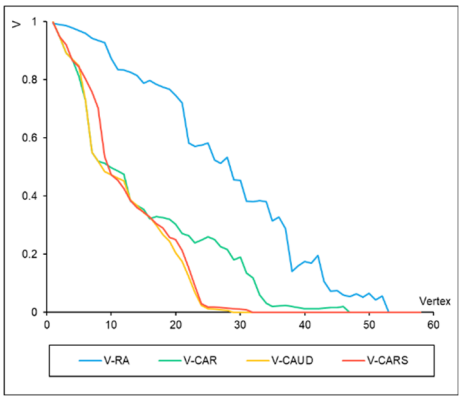

(h) ANet V

Figure 9. The robustness results of the single-mode network.

Comparing the four networks, HNet and RNet are deemed more robust than NNet and ANet. First, the speed of network failure varies among the networks. For HNet and RNet, the failure process can be divided into three stages: an initial rapid decrease in V, followed by a relatively high fluctuation stage and finally, another rapid decline. This suggests that the connectivity, completeness and uniformity of the network remain relatively stable during the second stage, even when a significant number of vertices are attacked. In contrast, NNet and ANet experience a rapid and continuous decrease in V throughout the attack, indicating a quick disintegration of the network structure upon damage.

Second, HNet and RNet exhibit a delayed failure compared to NNet and ANet. The average CR of HNet and RNet is 74.82 and 70.74%, respectively, which is higher than CR of NNet (68.01%) and ANet (66.81%). This suggests that HNet and RNet can withstand more severe attacks before reaching failure.

An intriguing phenomenon observed is the fluctuation plateau, which we refer to as the "city effect". When modeling the networks, the vertex IDs are sequentially arranged within the same city but adjacently arranged across different cities. Under CAR, the vertices are attacked consecutively based on their IDs when targeting vertices with the same degree. Consequently, the network within each city is destroyed, while the backbone network connecting the cities remains relatively intact,

resulting in the occurrence of a fluctuation plateau. However, the city effect does not prevent rapid failure under both CAUD and CARS since the network inside the cities and the backbone network are simultaneously destroyed. This city effect suggests that the network within each city is of lesser importance compared to the backbone network connecting the cities.

6.2. Robustness comparative analysis between CNet and the single-mode network

CNet exhibits better robustness under RA and CAR compared to CAUD and CARS. CR is 95.11 and 91.75% under RA and CAR respectively, which is significantly higher than CR under CAUD and CARS, which is 56.85 and 57.25%. Notably, the difference in robustness becomes particularly evident when considering the structural entropy. As mentioned in Section 5.2, CNet exhibits both random network and scale-free network properties. When the entropy decreases, the network structure transitions from disorder to a more ordered state. However, the robustness property can resist this change with stronger robustness offering greater resistance. In Figure 10(a), the green and blue dotted lines consistently fluctuate at a higher position for a longer period compared to the red and golden lines. This indicates that the resistance of entropy under RA and CAR is stronger, reflecting stronger robustness. Additionally, CNet also displays the city effect.

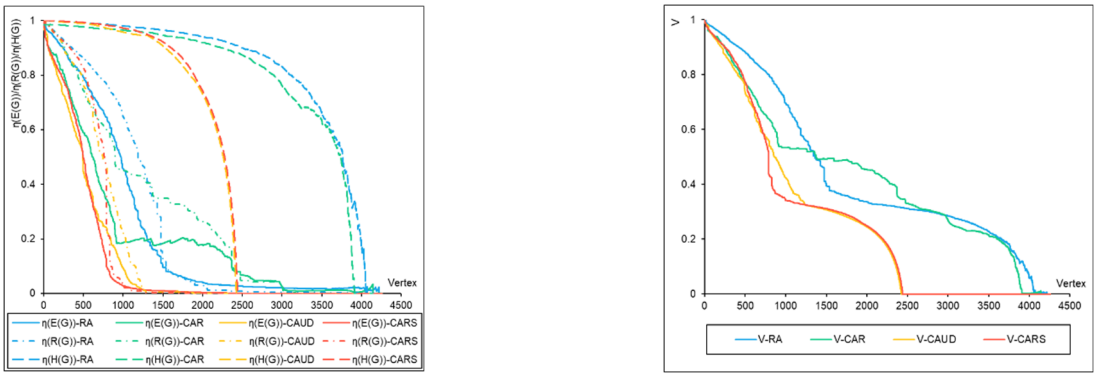

(a) $\eta(E(G))/\eta(R(G))/\eta(H(G))$ (b) V

Figure 10. The robustness results of CNet.

Figure 11 illustrates that the curves of CNet and HNet are similar regardless of the attack strategies and indicators. The original E of CNet is lower than that of RNet, NNet and ANet but slightly higher than that of HNet. This discrepancy arises because CNet has a larger number of vertices, resulting in longer average distances and lower global efficiency. However, the original R of CNet is slightly higher than that of HNet, indicating that the addition of other modes effectively increases connectivity.

Observing the changes in $\eta(E(G)), \eta(R(G)), \eta(H(G))$ and V, it is evident that regardless of the attack strategy, the curves of CNet are consistently higher than those of HNet. Furthermore, HNet reaches the critical point earlier than CNet, indicating that CNet is more robust than HNet. However, there is a brief period in the beginning under CARS when the V curve of HNet surpasses that of CNet. This phenomenon can be explained by two reasons: first, the original value of CNet is lower than that of HNet and second, due to the micronetwork of the transit hub, some high-degree vertices are replaced. At the initial stages of the attack, CNet lacks sufficient high-degree vertices to support

the overall network structure.

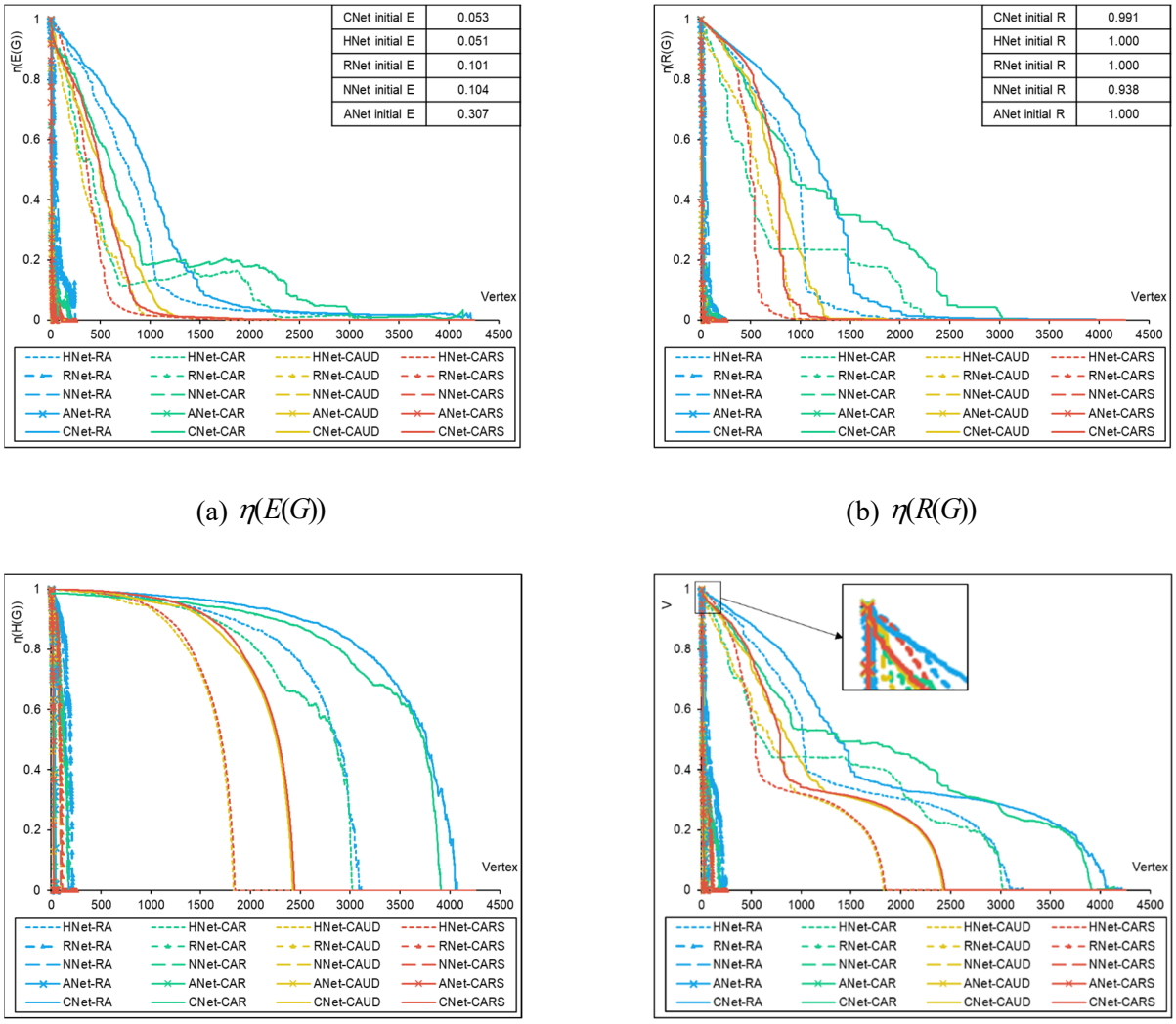

(a) $\eta(E(G))$ (b) $\eta(R(G))$

(c) $\eta(H(G))$ (d) V

Figure 11. Robustness comparative analysis.

7. Robustness analysis for CNets modeling by different methods

Three optimized modeling methods are proposed for the transfer network, the connecting road of the hub and the EEE. In this section, four contrast experiments are designed to explore the effect of these methods on network robustness and prove their validity. In each experiment, we compare the robustness of the two networks. All networks are derived from the Jiangsu Province data and use the same mapping rules. The robustness analysis is carried out according to four attack strategies.

Based on $R(G)$, two new indicators describe the robustness difference between networks G_1 and G_2 modeled by different methods.

The improved rate of the critical ratio (IRC). It describes the change in the critical rate of network failure under one attack mode. It can reflect changes in robustness without being affected by network size.

$$CR^R = \frac{CP^R}{N(G)} = \frac{\varphi(R(G) = 1/100R(G)^0)}{N(G)} \tag{17}$$

$$IRC = \frac{CR_1^R - CR_2^R}{CR_2^R} \times 100\% \tag{18}$$

CR_1^R and CR_2^R are separately denoted as critical ratios of G_1 and G_2 based on $R(G)$. If $IRC > 0$, the robustness of G_1 is better than that of G_2.

The improved rate of $R(G)$ (IRR). It describes the average difference in $R(G)$ between two networks before failure. It can reflect the differences in network connectivity when the same number of vertices are attacked.

$$\delta^j = \frac{(R(G_1)_j - R(G_2)_j)}{R(G_2)_j} \tag{19}$$

$$IRR = \frac{\sum_{j}^{\min(N_1^P, N_2^P)} \delta^j}{\min(N_1^P, N_2^P)} \times 100\% \tag{20}$$

$R(G_1)_j$ and $R(G_2)_j$ are denoted as $R(G)$ values of G_1 and G_2 when vertex j is attacked, respectively. δ^j is denoted as the improved rate of $R(G)$ when vertex j is attacked. If $IRR > 0$, the robustness of G_1 is better than that of G_2.

7.1. Influence of the mode transfer network on robustness

This experiment compares CNet and NTCNet (no transfer comprehensive transportation network). The core difference between them is the modeling method of hubs. CNet's mode transfer network inside the hub is constructed according to the optimized method. However, NTCNet uses one vertex to represent the hub according to the previous method [26,27], as shown in Figure 12.

(a) CNet (b) NTCNet

Figure 12. The modeling difference between CNet and NTCNet.

Table 5 shows that, compared with NTCNet, CNet can delay the critical point of network failure and this phenomenon is more significant under the calculated attack. Overall, the failure is delayed by an average of 2.79% under the four attack strategies. This shows that the transfer network inside the hub can improve the robustness of the network. Figure 13 shows that $\eta(R(G))$ of the two networks change synchronously at the beginning of the attack (0–500). Then, the gap of $\eta(R(G))$ experiences a process of first enlarging and then narrowing. Overall, under the four attack strategies, the average *IRR* is 52.95%. This indicates that under the same attack intensity, CNet can better maintain the network connectivity, which is 52.95% higher than NTCNet. The improvement is most significant in CARS, where *IRR* reaches 114.46%.

Table 5. *IRC* and *IRR* between CNet and NTCNet.

Attack mode	RA	CAR	CAUD	CARS	Average *IRC* and *IRR* of four attack strategies
CR_1^R (CNet)/%	59.83	75.76	30.91	27.91	
CR_2^R (NTCNet)/%	58.13	74.11	29.74	27.34	
IRC /%	2.92	2.22	3.95	2.07	2.79%
IRR /%	42.53	19.28	35.51	114.46	52.95%

The result indicates that CNet can more fully reflect the robustness of real networks than NTCNet. In addition, it also suggests that we should give more attention to the streamline design inside the hub, especially the physical separation design for the transfer between different directions. The separated transfer channel may reduce the probability of network damage. For example, for the security needs of major events such as the Olympic Games or the National People's Congress, travelers need to be checked. If the separation design is not made, all passengers' transfer channels must be blocked during screening so that the whole hub is paralyzed. If a separate design is made, only part of the transfer channel needs to be blocked and others still run. In this way, the harmful impact on the network is reduced, and robustness is improved.

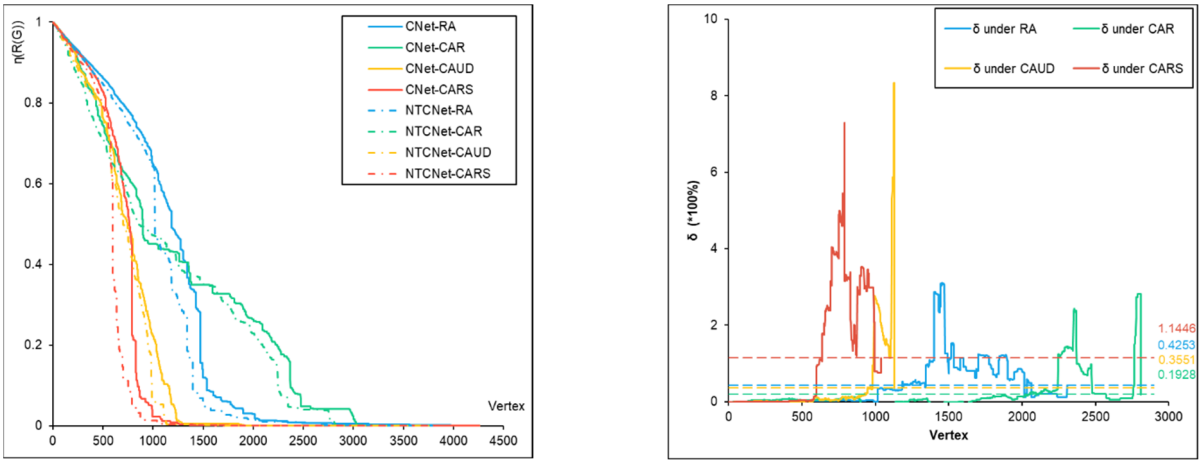

(a) $\eta(R(G))$ (b) Change of δ^j

Figure 13. The robustness comparison between CNet and NTCNet.

7.2. Influence of the connecting section on robustness

This experiment compares NTCNet and NCCNet (no connected comprehensive transportation network). The core difference between them is the modeling method of the connecting road outside the hub. In NTCNet, the hub is connected to the high-grade urban road by connecting section, but the hub is connected to the same road directly in NCCNet according to the previous method [26,28], as shown in Figure 14.

(a) NTCNet (b) NCCNet

Figure 14. The modeling difference between NTCNet and NCCNet.

Table 6 shows that, compared with NCCNet, NTCNet can delay the failure and the average *IRC* under the four attack strategies is 2.44%. The delay is most significant under CARS, with *IRC* reaching 4.94%. It is slightly different from the comparative combination of CNet and NTCNet. However, the *IRR* under RA is the lowest among all attack strategies, which is only 2.70%. It can be seen from Figure 15 that the $\eta(R(G))$ curves of NTCNet and NCCNet under RA are close and the maximum δ^j is only 0.8475, far lower than that of other attack strategies. It indicates that the robustness of NTCNet and NCCNet is close under RA. But under calculated attacks, things are different. The average *IRR* of the three calculated attacks is 42.49%, much higher than that of RA. Overall, the average *IRR* of all attack strategies is 32.54%. It indicates that, compared with NCCNet, NTCNet is more capable of maintaining network connectivity under attack, especially under calculated attack. In addition, since CNet is more robust than NTCNet, we can assume that CNet is much more robust than NCCNet.

Table 6. *IRC* and *IRR* between NTCNet and NCCNet.

Attack mode	RA	CAR	CAUD	CARS	Average *IRC* and *IRR* of four attack strategies
CR_1^R (NTCNet) /%	58.13	74.08	29.74	27.34	
CR_2^R (NCCNet) /%	56.31	73.42	29.55	26.05	
IRC /%	3.27	0.90	0.66	4.94	2.44%
IRR /%	2.70	85.55	13.89	28.02	32.54%

The result shows that CNet can best reflect the robustness of the real network, compared with NCCNet and NTCNet. It also shows that in modeling comprehensive transportation networks, it is necessary to express different networks and consider the connection between them. The connection

order of different grades of roads should not be ignored either. The result also reveals that when constructing a hub, it is necessary to avoid the direct connection between the high-grade roads and the hubs, or it will affect traffic organization and diversion management.

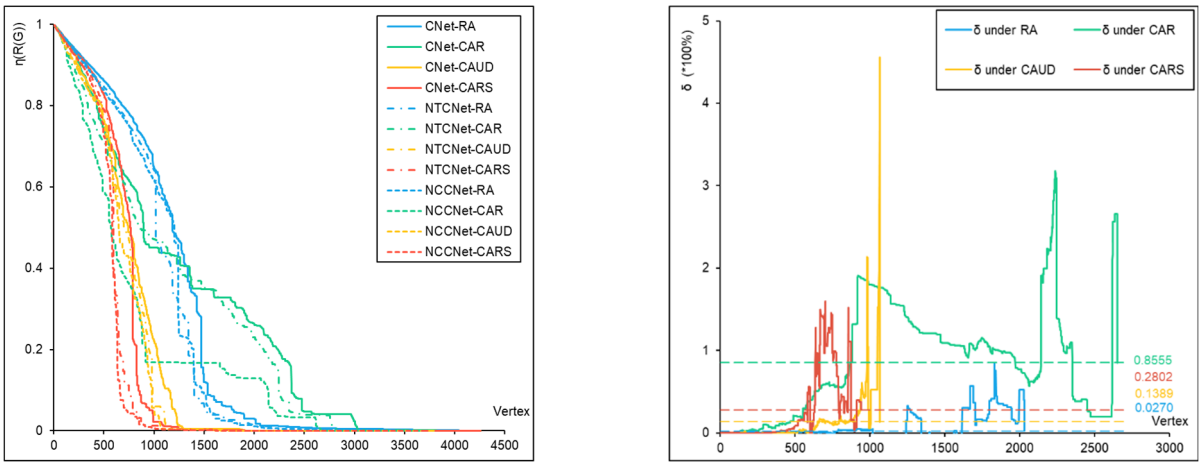

(a) $\eta(R(G))$ (b) Change of δ^j

Figure 15. The robustness comparison between NTCNet and NCCNet.

7.3. Influence of the number of optimized hubs on robustness

This experiment compares NCCNet and POCNet (partially optimized comprehensive network). POCNet means that only some hubs in NCCNet are optimized. Optimization refers to the construction of a mode transfer network inside the hub and the use of the connecting road outside the hub, as shown in Figure 16. Compared with CNet, NCCNet and NTCNet, POCNet has stronger practical significance. In reality, resources are limited and it is usually difficult to optimize all hubs. When the number of optimized hubs is different, how will the robustness of the network be influenced? This experiment will answer this question.

(a) Optimized hub (b) Unoptimized hub

Figure 16. The modeling difference between the optimized and unoptimized hub.

In this experiment, POCNet is obtained by randomly optimizing different proportions of hubs in

NCCNet. For 211 hub nodes in NCCNet, we design 10 groups of experiments. In each group, the proportion of optimized hubs is α, $\alpha = 10\%, 20\%, ..., 100\%$. To eliminate the uncertainty caused by random selection, 10 parallel experiments are conducted for each group. In each parallel experiment, a hub with a random proportion of α was selected for optimization. The average value of *IRC* and *IRR* of 10 parallel experiments was calculated as the result of this group. It is worth noting that POCNet and CNet are the same when $\alpha = 100\%$.

Table 7. *IRC* and *IRR* between POCNet and CNet.

α	RA			CAR			CAUD			CARS			Average values of four attacks	
POCNet	CR^R/%	*IRC* /%	*IRR* /%	CR^R/%	*IRC* /%	*IRR* /%	CR^R/%	*IRC* /%	*IRR* /%	CR^R/%	*IRC* /%	*IRR* /%	*IRC* /%	*IRR* /%
NCCNet	56.31	0	0	73.44	0	0	29.55	0	0	26.06	0	0	0	0
10%	58.99	4.76	23.54	73.77	0.45	14.87	29.67	0.40	3.08	26.45	1.49	26.71	1.78	17.05
20%	60.55	7.54	30.86	73.81	0.50	16.75	29.95	1.36	9.44	26.70	2.46	40.89	2.96	24.48
30%	58.02	3.05	22.67	74.31	1.18	32.19	30.11	1.88	13.18	26.54	1.84	39.56	1.99	26.90
40%	58.84	4.50	40.67	74.53	1.48	35.98	30.20	2.19	21.57	26.36	1.14	71.27	2.33	42.37
50%	58.60	4.07	38.17	74.67	1.67	56.70	30.35	2.69	26.03	26.77	2.71	79.49	2.78	50.10
60%	55.22	-1.93	26.87	74.97	2.08	68.72	30.69	3.85	39.52	27.02	3.68	115.59	1.92	62.68
70%	57.91	2.84	32.92	75.35	2.61	88.61	30.63	3.64	41.32	27.08	3.91	151.08	3.25	78.48
80%	55.79	-0.92	31.25	75.31	2.54	96.13	30.78	4.14	47.96	26.77	2.73	162.62	2.12	84.49
90%	56.15	-0.28	38.40	76.27	3.85	126.77	31.09	5.20	63.61	26.77	2.73	169.57	2.88	99.59
100% (CNet)	59.83	6.25	42.45	76.26	3.84	146.72	31.12	5.29	73.77	28.09	7.79	195.30	3.87	114.56

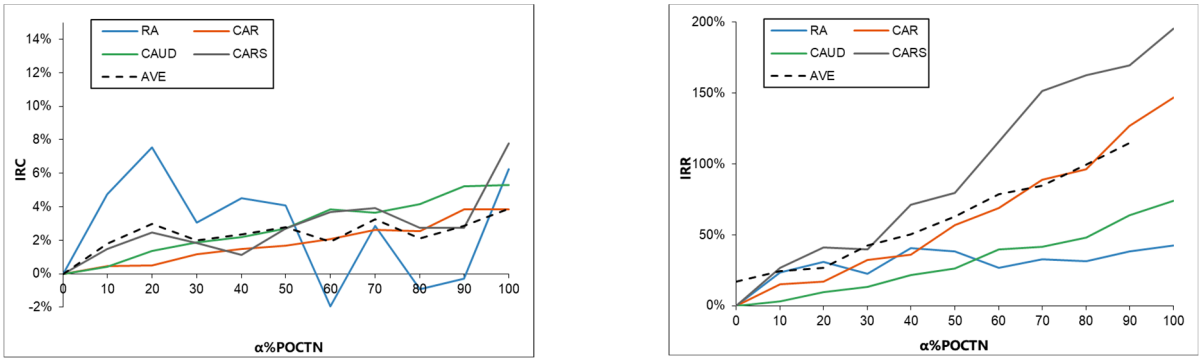

(a) *IRC* (b) *IRR*

Figure 17. Changes in *IRC* and *IRR* with different α

Table 7 and Figure 17 shows that for different α, the values of *IRC* and *IRR* are positive under the four attack modes. With the increase in α, *IRR* shows a steadily increasing trend from 17.05% to 114.56%. At the same time, *IRC* fluctuates between 1.78 and 3.87%. However, for different types of attack, *IRC* and *IRR* behave differently. Under CAR, CAUD and CARS, *IRC* and *IRR* gradually increase with increasing α. However, under RA, *IRC* shows great fluctuations, even less than zero and *IRR* fluctuates by approximately 30%. This fluctuation can be more intuitively illustrated in

Figure 18. The curves in Figure 18(a) show irregular fluctuations with different α. For example, when $\alpha = 90\%$, the curve fluctuates wildly between 0–180%. In Figure 18(b)–(d), the curve presents a consistent fluctuation rule and the larger α is, the larger the value represented by the curve.

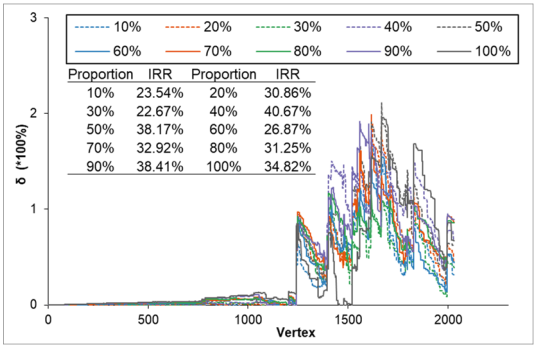

(a) Change of δ^j under RA

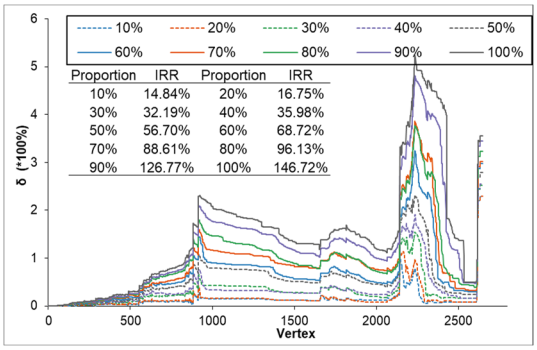

(b) Change of δ^j under CAR

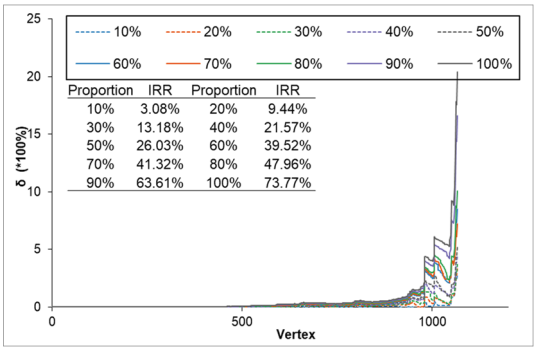

(c) Change of δ^j under CAUD

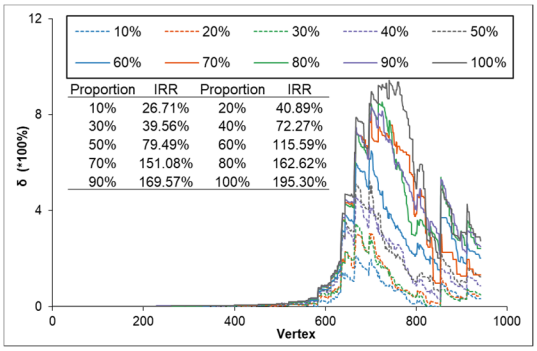

(d) Change of δ^j under CARS

Figure 18. Change of δ^j with different α.

The results show that POCNet is more robust than NCCNet overall. This robustness enhancement is more significant under calculated attacks but less significant under random attacks. Under a calculated attack, the robustness of POCNet increases with increasing α, but under a random attack, the robustness of POCNet fluctuates at a lower level.

From a practical point of view, optimized hubs can effectively resist the risks brought by calculated attacks and the more optimized hubs there are, the stronger the robustness. However, the improvement effect of such optimization on robustness under random attacks is not significant.

7.4. Influence of EEE modeling method on robustness

This experiment compares HNet and NRHNet (no ramp highway network). The core difference between them is the modeling method of EEE. In HNet, the EEE is represented by three vertices and two edges according to the optimized method but by only one vertex in NRHNet according to the previous method [64], as shown in Figure 19.

(a) HNet (b) NRHNet

Figure 19. The modeling difference between HNet and NRHNet

Table 8 shows under the four attack strategies, the average *IRC* is 12.34%. It indicates that HNet can withstand more severe attacks than NRHNet. Figure 20 shows the change of $\eta(R(G))$ and δ^j under four attack strategies. Four dash lines in Figure 20(b) represent the average *IRR* values under each attack strategy. At the beginning of the attack, $\eta(R(G))$ of two networks keep changing synchronously. Then, $\eta(R(G))$ of HNet is gradually larger than NRHNet and the gap becomes more apparent. Finally, the gap narrows. However, under CAUD the gap of $\eta(R(G))$ reaches its peak at the CP^R. Overall, the average *IRR* under the four attack strategies is 265.69%. It indicates that HNet can better maintain network connectivity under the same attack. Therefore, both *IRC* and *IRR* indicate that HNet is more robust than NRHNet.

Table 8. *IRC* and *IRR* between HNet and NRHNet.

Attack mode	RA	CAR	CAUD	CARS	
CP_1^R (HNet)/%	61.55	78.34	33.40	30.72	Average *IRC* and *IRR* of four attack strategies
CP_2^R (NRHNet)/%	55.68	71.24	28.85	25.45	
IRC /%	22.10	22.74	16.58	11.84	12.34%
IRR /%	135.73	739.49	142.93	44.61	265.69%

The reason is that EEE in NRHNet is represented as a vertex with a degree value of 4 or higher. Compared with HNet, NRHNet has fewer vertices but more high-degree vertices. When the same number of vertices is attacked, the high-degree vertices in NRHNet are more likely to be destroyed, which damages the network structure.

The result indicates that the modeling optimization method for EEE is more valuable than the previous method. On the one hand, the previous method underestimates the robustness of HNet, but the optimized method can illustrate it well. On the other hand, the stronger robustness of HNet verifies the rationality of ramp construction in reality and demonstrates the vital role of ramps in highway network modeling.

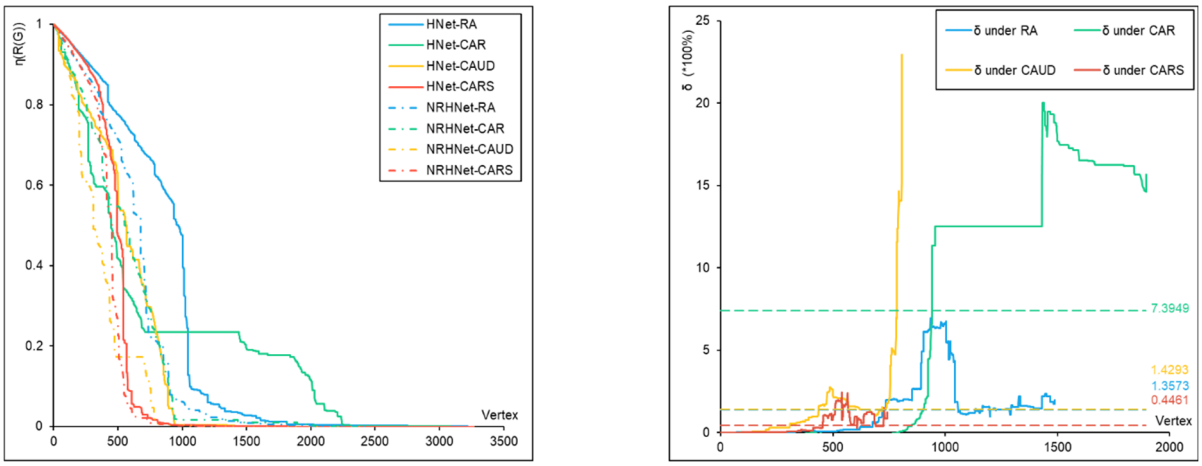

(a) $\eta(R(G))$ (b) Change of δ^j

Figure 20. The robustness comparison between HNet and NRHNet.

8. Conclusions

The comprehensive transportation network improves commuting efficiency and promotes economic development. A comprehensive transportation network design often considers travel behavior and local geological features. Therefore, it is naturally of great importance to explore the structural characteristics of a multimodal comprehensive transportation network. In this paper, five networks are modeled using an optimized modeling method and taking Jiangsu Province as an example case. In particular, CNet focuses on the mode transfer process at the transit hub. Then, some characteristics are explored.

For statistical characteristics, we find that CNet, HNet, RNet and NNet are not scale-free networks and do not have small-world properties, but ANet is the opposite. Although HNet is the main component of CNet from the numerical view of vertex and edge, the CNet's average distance is shorter and the cluster degree is higher than HNet. It shows that CNet is tighter. In addition, there is another interesting finding that the vertex with a degree of three occupies a high ratio.

For robustness characteristics, we find that the robustness is different under different attack strategies, but CNet is more robust than the other four single-mode networks regardless of the attack strategy. Under RA, the five networks are all robust. However, their capabilities against failure are different during the attack process. Under CAR, they are all robust. HNet and CNet are more robust due to the city effect. Under CAUD and CARS, they are not sufficiently robust.

For the influence on robustness and the validity of the optimized modeling method, we find that all three optimized methods for hubs and EEE can enhance network robustness compared with the other modeling methods. The average critical rate of network failure (*IRC*) is delayed by 12.34, 2.79 and 2.44% and the average connectivity degree (*IRR*) of the network is increased by 265.69, 52.95 and 32.54%. In addition, the more hubs that are optimized, the stronger the overall robustness of the network. This trend is even more pronounced under calculated attacks. This reveals that the hub and EEE are essential in the comprehensive transportation network. Hubs and EEE with powerful transfer capabilities can improve robustness.

From the research results, we would like to offer some suggestions to CNet from the planning, construction and management points of view. In the planning stage, more transit hubs should be designed to enhance the scale-free and small-world properties of CNet. More hubs can make the network tighter, which can shorten the travel space distance and provide more paths for the traveler. In the construction stage, a transit hub with powerful transfer facilities is recommended. For example, the transfer channel with a physical separation design between different directions is better than the mixed channel. This design not only makes the transfer faster but also greatly improves the robustness of CNet. Under a special background, the design can maintain the smooth operation of the system and minimize losses. For instance, passengers from certain directions are not allowed to transfer at the hub during events such as the Olympic Games. At this time, only a part of the transfer channels is restricted instead of all channels being closed. In the management stage, a more sophisticated modeling method should be considered when evaluating the robustness of CNet. If EEE and the hub are not modeled factually and elaborately, the robustness of the real transportation system may be underestimated, which is not conducive to accurate evaluation results. Our modeling method provides an effective solution and it is well demonstrated.

However, there are still shortcomings in this article. This article only analyzes the infrastructure network. In addition, the robustness analysis remains at the static level and does not consider the capacity of vertices and edges. Future research on operation and weighted comprehensive transportation networks can be carried out.

Use of AI tools declaration

The authors declare they have not used Artificial Intelligence (AI) tools in the creation of this article.

Acknowledgments

This research is supported by the key project of National Natural Science Foundation of China (51878166) and “Zhishan” Scholars Programs of Southeast University.

Conflict of interest

The authors declare there is no conflict of interest.

References

1. W. Wang, X. D. Hua, Y. T. Zheng, Multi-network integrated traffic analysis model and algorithm of comprehensive transportation system, *J. Traffic Transp. Eng.*, **21** (2021), 159–172. https://doi.org/10.19818/j.cnki.1671-1637.2021.02.014
2. R. Albert, H. Jeong, A. L. Barabási, Internet-Diameter of the world wide web, *Nature*, **401** (1999), 130–131. https://doi.org/10.1136/tc.12.3.256
3. A. L. Brabasi, *Network Science*, Cambridge University Press, Cambridge, United Kingdom, 2016.

4. C. von Ferber, T. Holovatch, Y. Holovatch, V. Palchykov, Network harness: Metropolis public transport, *Phys. A*, **380** (2007), 585–591. https://doi.org/ 10.1016/J.PHYSA.2007.02.101
5. C. von Ferber, T. Holovatch, Y. Holovatch, V. Palchykov, Public transport networks: empirical analysis and modeling, *Eur. Phys. J. B*, **68** (2009), 261–275. https://doi.org/10.1140/EPJB/E2009-00090-X
6. F. Du, H. W. Huang, D. M. Zhang, F. Zhang, Analysis of characteristics of complex network and robustness in Shanghai metro network, *Eng. J. Wuhan Univ.*, **49** (2016), 701–707. https://doi.org/10.14188/j.1671-8844.2016-05-010
7. J. Y. Lin, Y. F. Ban, Complex network topology of transportation systems, *Transport Rev.*, **33** (2013), 658–685. https://doi.org/10.1080/01441647.2013.848955
8. M. Kurant, P. Thiran, Extraction and analysis of traffic and topologies of transportation networks, *Phys. Rev. E*, **74** (2006), 036114. https://doi.org/10.1103/PhysRevE.74.036114
9. S. Porta, P. Crucitti, V. Latora, The network analysis of urban: A primal approach, *Environ. Plann. B: Urban Anal. City Sci.*, **33** (2006), 705–725. https://doi.org/10.1068/b32045
10. S. H. Dau, O. Milenkovic, Inference of latent network features via co-intersection representations of graphs, in *2016 IEEE International Symposium on Information Theory*, (2016), 1351–1355.
11. R. Wang, X. Cai, Hierarchical structure, disassortativity and information measures of the US flight network, *Chin. Phys. Lett.*, **22** (2005), 2715–2718.
12. W. Li, X. Cai, Statistical analysis of airport network of China, *Phys. Rev. E*, **69** (2004), 046106. https://doi.org/10.1103/PhysRevE.69.046106
13. P. R. V. Boas, F. A. Rodriguesa, L. D. Costa, Modeling worldwide highway networks, *Phys. Lett. A*, **374** (2009), 22–27. https://doi.org/10.1016/j.physleta.2009.10.028
14. C. E. Mandl, Evaluation and optimization of urban public transportation networks, *Eur. J. Oper. Res.*, **5** (1980), 396–404. https://doi.org/10.1016/0377-2217(80)90126-5
15. V. Latora, M. Marchiori, Is Boston subway a small-world network?, *Phys. A*, **314** (2002), 109–113. https://doi.org/10.1016/S0378-4371(02)01089-0
16. A. Chen, H. Yang, H. K. Lo, W. H. Tang, A capacity related reliability for transportation networks, *J. Adv. Transp.*, **33** (1999), 183–200. https://doi.org/10.1002/atr.5670330207
17. T. Y. Chen, H. L. Chang, G. H. Tzeng, Using a weight assessing model to identify route choice criteria and information effects, *Transp. Res. Part A Policy Pract.*, **35** (2001), 197–224. https://doi.org/10.1016/S0965-8564(99)00055-5
18. C. M. Zhang, W. Q. Wang, W. T. Li, W. L. Xiang, Analysis on regional economic characters of Lan-Xin High Speed Railway based on panel data, *J. Rail Way Sci. Eng.*, **14** (2017), 12–18. https://doi.org/10.19713/j.cnki.43-1423/u.2017.01.003
19. O. Froidh, Perspectives for a future high-speed train in the Swedish domestic travel market, *J. Transp. Geogr.*, **16** (2008), 268–277. https://doi.org/10.1016/j.jtrangeo.2007.09.005
20. M. T. Trobajo, M. V. Carriegos, Spanish airport network structure: Topological characterization, *Comput. Math. Methods*, **2022** (2022), 4952613. https://doi.org/10.1155/2022/4952613
21. Y. M. Zhou, J. W. Wang, G. Q. Huang, Efficiency and robustness of weighted air transport networks, *Transp. Res. Part E Logist. Transp. Rev.*, **122** (2019), 14–26. https://doi.org/10.1016/j.tre.2018.11.008

22. J. H. Zhang, F. N. Hu, S. L. Wang, Y. Dai, Y. X. Wang, Structural vulnerability and intervention of high speed railway networks, *Phys. A*, **462** (2016), 743–751. https://doi.org/10.1016/j.physa.2016.06.132
23. P. Sen, S. Dasgupta, A. Chatterjee, P. A. Sreeram, G. Mukherjee, S. S. Manna, Small-world properties of the Indian railway network, *Phys. Rev. E*, **67** (2003), 036106. https://doi.org/10.1103/PhysRevE.67.036106
24. G. Bagler, Analysis of the airport network of India as a complex weighted network, *Phys. A*, **387** (2008), 2972–2980. https://doi.org/10.1016/j.physa.2008.01.077
25. J. Sienkiewicz, J. A. Hołyst, Statistical analysis of 22 public transport networks in Poland, *Phys. Rev. E*, **72** (2005), 046127. https://doi.org/10.1103/PhysRevE.72.046127
26. P. Marcotte, Supernetworks: Decision-making for the information age, *J. Reg. Sci.*, **43** (2003), 615–617.
27. S. C. Dafermos, The traffic assignment problem for multiclass-user transportation networks, *Transp. Sci.*, **6** (1972), 73–87. https://doi.org/10.1287/trsc.6.1.73
28. Z. X. Wu, W. H. K. Lam, Network equilibrium model for congested multi-mode transport network with elastic demand, *J. Adv. Transp.*, **37** (2003), 295–318. https://doi.org/10.1002/atr.5670370304
29. P. Xu, Intercity multi-modal traffic assignment model and algorithm for urban agglomeration considering the whole travel process, in *IOP Conference Series: Earth and Environmental Science*, **189** (2018), 062016. https://doi.org/10.1088/1755-1315/189/6/062016
30. H. Y. Ding, *Research on Urban Multi-Modal Public Transit Network Fast Construction Method and Assignment Model*, Ph.D thesis, Southeast University, 2018.
31. A. Lozano, G. Storchi, Shortest viable path algorithm in multimodal networks, *Transp. Res. Part A Policy Pract.*, **35** (2001), 225–241. https://doi.org/10.1016/S0965-8564(99)00056-7
32. H. P. Shi, J. Lu, Z. Z. Yang, A super-network model based analysis of effect of comprehensive transportation polices, *Logist. Technol.*, **31** (2012), 12–15. https://doi.org/10.3969/j.issn.1005-152X.2012.07.005
33. G. H. Deng, M. Zhong, A. Raza, J. D. Hunt, Y. Zhou, A methodological study of multimodal freight transportation models for large regions based on an integrated modeling framework, *J. Transp. Syst. Eng. Inf. Technol.*, **22** (2022), 30–42. https://doi.org/10.16097/j.cnki.1009-6744.2022.04.004
34. J. Xu, Y. N. Yin, X. Wen, G. Z. Lin, Research on the supernetwork equalization model of multilayer attributive regional logistics integration, *Discrete Dyn. Nat. Soc.*, **2019** (2019), 8583060. https://doi.org/10.1155/2019/8583060
35. Y. Luo, D. L. Qian, Construction of subway and bus transport networks and analysis of the network topology characteristics, *J. Transp. Syst. Eng. Inf. Technol.*, **15** (2015), 39–44. https://doi.org/10.16097/j.cnki.1009-6744.2015.05.006.
36. F. Xu, J. F. Zhu, W. D. Yang, Construction of high-speed railway and airline compound network and the analysis of its network topology characteristics, *Complex Syst. Complexity Sci.*, **10** (2013), 1–11. https://doi.org/10.13306/j.1672-3813.2013.03.001
37. X. Feng, S. W. He, G. Y. Li, J. S. Chi, Transfer network of high-speed rail and aviation: Structure and critical components, *Phys. A*, **581** (2021), 126197. https://doi.org/10.1016/j.physa.2021.126197

38. M. Ouyang, Z. Z. Pan, L. Hong, Y. He, Vulnerability analysis of complementary transportation systems with applications to railway and airline systems in China, *Reliab. Eng. Syst. Saf.*, **142** (2015), 248–257. https://doi.org/10.1016/j.ress.2015.05.013
39. Y. Luo, D. L. Qian, Construction of subway and bus transport networks and analysis of the network topology characteristics, *J. Transp. Syst. Eng. Inf. Technol.*, **15**(2015), 39–44. https://doi.org/10.16097/j.cnki.1009-6744.2015.05.006
40. X. H. Li, J. Y. Guo, C. Gao, Z. Su, D. Bao, Z. L. Zhang, Network-based transportation system analysis: A case study in a mountain city, *Chaos, Solitons Fractals*, **107** (2018), 256–265. https://doi.org/10.1016/j.chaos.2
41. G. Liu, Y. S. Li, Robustness analysis of railway transer system based on complex network theory, *Appl. Res. Comput.*, **31** (2014), 2941–2942, 2973. https://doi.org/10.3969/j.issn.1001-3695.2014.10.013
42. S. Wandelt, X. Shi, X. Q. Sun, Estimation and improvement of transportation network robustness by exploiting communities, *Reliab. Eng. Syst. Saf.*, **206** (2021), 107307. https://doi.org/10.1016/j.ress.2020.107307
43. M. Barthélemy, Betweenness centrality in large complex networks, *Eur. Phys. J. B*, **38** (2004), 163–168. https://doi.org/10.1140/epjb/e2004-00111-4
44. U. Demšar, O. Špatenková, K. Virrantaus, Identifying critical locations in a spatial network with graph theory, *Trans. GIS*, **12** (2008), 61–82. https://doi.org/10.1111/j.1467-9671.2008.01086.x
45. Y. S. Chen, X. Y. Wang, X. W. Song, J. L. Jia, Y. Y. Chen, W. L. Shang, Resilience assessment of multimodal urban transport networks, *J. Circuits Syst. Comput.*, **31** (2022), 18. https://doi.org/10.1142/S0218126622503108
46. Y. Y. Duan, F. Lu, Robustness of city road networks at different granularities, *Phys. A*, **411** (2014), 21–34. https://doi.org/10.1016/j.physa.2014.05.073
47. F. Morone, H. A. Makse, Influence maximization in complex networks through optimal percolation, *Nature*, **524** (2015), 65–68. https://doi.org/10.1038/nature14604
48. L. Zdeborová, P. Zhang, H. J. Zhou, Fast and simple decycling and dismantling of networks, *Sci. Rep.*, **6** (2016), 37953. https://doi.org/10.1038/srep37954
49. O. Cats, G. J. Koppenol, M. Warnier, Robustness assessment of link capacity reduction for complex networks: Application for public transport systems, *Reliab. Eng. Syst. Saf.*, **167** (2017), 544–553. https://doi.org/10.1016/j.ress.2017.07.009
50. W. L. Shang, Z. Y. Gao, N. Daina, H. R. Zhang, Y. Long, Z. L. Guo, et al., Benchmark analysis for robustness of multi-scale urban road networks under global disruptions, *IEEE Trans. Intell. Transp. Syst.*, **2022** (2022). https://doi.org/10.1109/TITS.2022.3149969
51. M. Ouyang, C. Liu, M. Xu, Value of resilience-based solutions on critical infrastructure protection: Comparing with robustness-based solutions, *Reliab. Eng. Syst. Saf.*, **190** (2019), 106506. https://doi.org/10.1016/j.ress.2019.106506
52. A. Kermanshah, S. Derrible, A geographical and multi-criteria vulnerability assessment of transportation networks against extreme earthquakes, *Reliab. Eng. Syst. Saf.*, **153** (2016), 39–49. https://doi.org/10.1016/j.ress.2016.04.007
53. W. L. Shang, Y. Y. Chen, C. C. Song, W. Y. Ochieng, Robustness analysis of urban road networks from topological and operational perspectives, *Math. Probl. Eng.*, **2020** (2020), 5875803. https://doi.org/10.1155/2020/5875803

54. Z. Z. Liu, H. Chen, E. Z. Liu, W. Y. Hu, Exploring the resilience assessment framework of urban road network for sustainable cities, *Phys. A*, **586** (2022), 126465. https://doi.org/10.1016/j.physa.2021.126465
55. Y. F. Zhang, S. T. Ng, Robustness of urban railway networks against the cascading failures induced by the fluctuation of passenger flow, *Reliab. Eng. Syst. Saf.*, **219** (2022), 108227. https://doi.org/10.1016/j.ress.2021.108227
56. Y. Chen, J. E. Wang, F. J. Jin, Robustness of China's air transport network from 1975 to 2017, *Phys. A*, **539** (2020), 122876. https://doi.org/10.1016/j.physa.2019.122876
57. T. Li, L. L. Rong, K. S. Yan, Vulnerability analysis and critical area identification of public transport system: A case of high-speed rail and air transport coupling system in China, *Transp. Res. Part A Policy Pract.*, **127** (2019), 55–70. https://doi.org/10.1016/j.tra.2019.07.008
58. Available from: https://navinfo.com/en/aboutus.
59. *Air Traffic Management Office*, Specifications for the Compilation and Drawing of Civil Aviation Instrument Route Charts and Area Charts, Available from: http://www.caac.gov.cn/XXGK/XXGK/GFXWJ/202111/t20211130_210338.html.
60. H. Li, L. X. Gan, Y. Z. Zheng, Y. Q. Wen, Complexity of waterway networks in port waters, *J. Navig. China*, **38** (2015), 94–98, 130. https://doi.org/10.3969/j.issn.1000-4653.2015.03.021
61. N. Y. Lou, C. H. Huang, Y. L. Chen, Y. Luan, J. H. Yuan, Network characteristics and robustness analysis of high level waterway network in the Yangtze River Delta, *J. Dalian Marit. Univ.*, **47** (2021), 28–36. https://doi.org/10.16411/j.cnki.issn1006-7736.2021.01.004.
62. B. B. Fu, Z. Y. Gao, F. S. Liu, X. J. Kong, Express passenger transport system as a scale-free network, *Mod. Phys. Lett. B*, **20** (2006), 1755–1761. https://doi.org/10.1142/S0217984906011803
63. W. Zhao, H. S. He, Z. C. Lin, K. Q. Yang, The study of properties of Chinese railway passenger transport network, *Acta Phys. Sin.*, **55** (2006), 3906–3911. https://doi.org/10.7498/aps.55.3906
64. L. N. Wu, Y. F. Lyu, Y. S. Ci, Connectivity reliability for provincial freeway network: A case study in Heilongjiang, China, *J. Transp. Syst. Eng. Inf. Technol.*, **18** (2018), 134–140. https://doi.org/10.16097/j.cnki.1009-6744.2018.Sup.1.020

AIMS Press